Chapter 5

Photoswitchable Foldamers

Introduction of photochromic azobenzene units into helically folding, amphiphilic oligo (*meta*-phenylene ethynylene)s leads to photocontrol over the helix-coil transition in this important class of foldamers. Two design principles have been followed by introducing *cis*- or *trans*-azobenzene units in the folding backbone to either selectively turn the helical state on or off. Several oligomer series have been synthesized and investigated with regard to their folding behavior in both dark and irradiated states.

Part of this work has been published: (a) *Polym. Prep*. **2005**, *46*, 161. (b) *Angew. Chem*. in press.

Introduction

Recent years have witnessed enormous progress in the design of artificial backbones capable to adopt well-defined secondary structures, in particular of the helix type, in solution.[1] The helical folding process is governed by non-covalent interactions such as hydrogen-bonding, metal coordination, electrostatic and π,π-stacking interactions among others. Therefore, the helix-coil transition is most frequently induced by increasing the temperature, changing solvent composition or adding denaturants. Such denaturation experiments provide insight into the stability of the helical conformation and the cooperativity involved in the folding process. However, methods to control this important conformational transition using light as perhaps the most convenient external stimulus have been limited. Photochromic molecules,[2] displaying two independently addressable switching states, have been used to affect structure and function at the molecular level.[3]

Photochromic molecules have been used to control the helix-coil transition in various polypeptide backbones.[4] Thereby, two approaches have been followed. 1) *Side chain approach*: in this approach photochromic molecules have been introduced as side chains to the polypeptide

backbones. For example spiropyran units have been incorporated as side chains to poly(L-glutamic acid). Photoisomerization of these units results in the conformational transition of the poly(L-glutamic acid) backbone from a random coil to a helical structure.[5] Similarly, azobenzene units have been attached as side chains to poly(L-glutamic acid). Irradiation results in conformational transition of the random coil backbone to a helical structure.[6] Poly (L-lysine) appended with azobenzene chromophore is shown to transform from a β-sheet structure to an α-helix when photoisomerized.[7] The remarkable conformational transitions in all of these cases were found to be very dependent on the polymer surrounding and solvent mixtures and hence were attributed to the changes in the polarity of the photochromic molecule and its interaction with the surrounding media. 2) *Tether approach*: in this approach, the azobenzene unit is used as a cross-linker between two different (cysteine) segments of a peptide backbone.[8] In one case, the photochromic molecule links the i and i+4 cysteine groups and photogeneration of the *cis*-azobenzene favors a helical backbone conformation. In other case, the azobenzene unit connects the i and i+11 cysteine residues and in this case of *trans*- to *cis*- isomerization destabilizes the helical conformation. Thereby, the helix content of a peptide is shown to be controlled by photoisomerization of an azobenzene moiety.[9]

However, there are no examples of photochromic molecules incorporated in to the helical backbone for governing the helix-coil equilibrium. We wished to incorporate photoswitchable units in the folding back bone so that geometric changes due to photoisomerization in the chromophore can be used to control the helix-coil transition.

Choice of the Stimulus

The use of light as stimulus is particularly attractive. Its non-invasive nature, the ease to control and dose, and absence of waste byproducts makes it the stimulus of choice. The rapid photochemical reactions offer means to bring about the desired change very quickly and hence a fast response can be obtained from the system.

Choice of the Photochromic Moiety

The choice of the photochromic unit is quite important. Ideally, it should be easily synthesized and capable of undergoing large changes of its molecular geometry during switching. The photoreaction should be easily monitored by spectroscopic methods and allow to be repeated many times. The azobenzene group suits this purpose very well, as the reversible *trans-cis* photo-isomerization of azobenzene is known to be one of the cleanest photoreactions that proceed with

large structural change in the geometry of the chromophore. This process gives rise to the possibility of controlling the conformation and therefore functions of compounds containing azobenzene by using light as an external stimulus. The disadvantage of using azobenzene originates from the incomplete isomerization, i.e. both *cis*- and *trans*- isomers are present in the photostationary state (PSS).

Choice of the Folding Backbone

Oligo (*m*-phenylene ethynylene)s are known to adopt a helical conformation in polar solvents.[10] The driving force for such folding reaction is the solvophobicity of the relatively non-polar backbone in the polar environment and favorable π,π–stacking interactions between the neighboring electron-deficient aromatic repeat units. The *meta*-connectivity of the repeat unit allows the molecule to fold back on itself when it is of sufficient length (n > 8) leading to helical structure[11], where six repeat units constitute a turn.[12] Quantitative analysis of absorption and fluorescence data shows a linear relationship between chain length and helix stabilization energy.[11]

The helix-coil transition in oligo (*m*-phenylene ethynylene) foldamers is governed by the quality of solvent[13], temperature[14], metal complexation[15] and hydrogen bonding[16] However, so far now no photocontrol over the folding transition has been achieved within these artificial helically folding systems. We aimed to achieve this goal by incorporating a photochromic molecule into the helical backbone such that light controls the helix-coil transition, as illustrated in Figure 1.

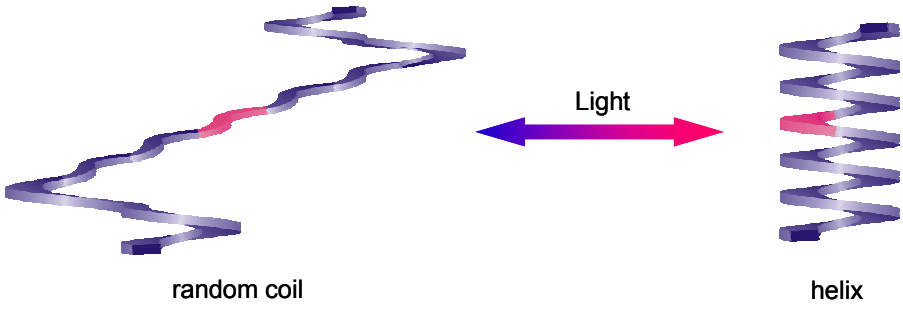

Figure 1. Photocontrol of the helix-coil transition in helical foldamers.

Design Principle

Our working hypothesis is to replace a single internal diphenylacetylene unit by differently substituted *trans*-azobenzene chromophores (Figure 2). Thereby, either (thermally) stable helices or coils should be accessible and hence the helical conformation could be turned off

or on using irradiation. The length of the oligomeric sequences attached to the photochromic unit has to be adjusted in such way that they cannot adopt a stable helical conformation by themselves but isomerization either breakes or creates a kinked connection to lead to helix denaturation or formation.

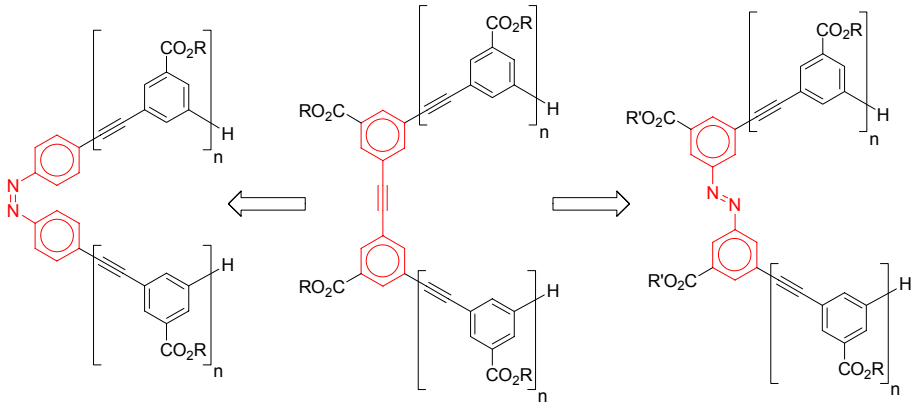

Figure 2. Structural resemblance of *para*-substituted *cis*-azobenzene (left) and *mata*-substituted *trans*-azobenzene (right) chromophores to the diphenylacetylene unit of the oligo(*m*-phenylene ethynylene)s foldamer.

Turn-on helices

We anticipated that incorporation of a *para*-substituted *trans*-azobenzene core in oligo (*m*-phenylene ethynylene) foldamers would furnish a random coil due to the linear geometry of the substituent at *para* position. *Trans-cis* photoisomerization should trigger the folding reaction as the curved geometry of the *cis*-isomer would provide the necessary kink in the structure needed to allow the molecule to fold on itself in polar environments (Figure 3).

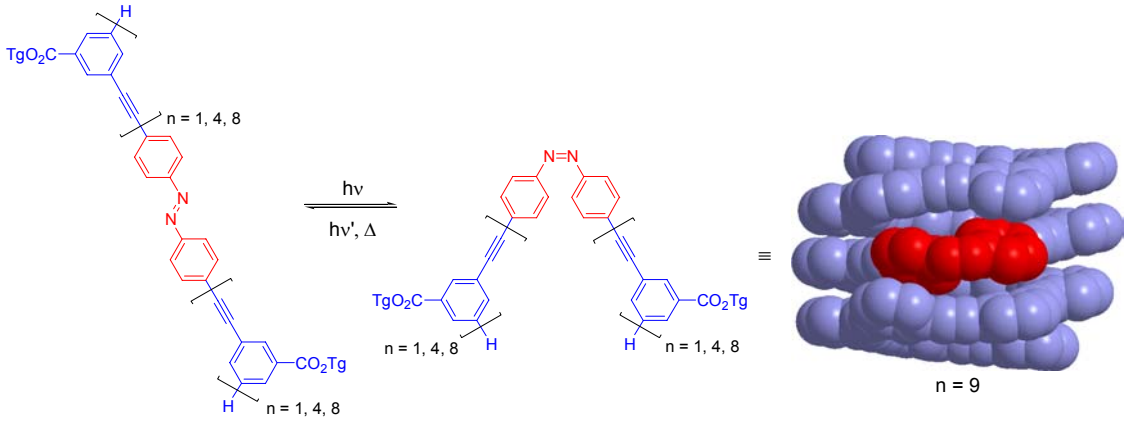

Figure 3. Photoisomerization of the oligo(*m*-phenylene ethynylene)s foldamer containing a *para*-substituted azobenzene core (left). A space filling model showing the expected helical conformation of oligomer **12** as a result of *trans-cis* photoisomerization.

Oligomers of different lengths were synthesized. Oligomers **11** and **12** have 5 and 9 repeat units attached to each side of the azobenzene chromophore, respectively. The minimum number of repeat units required to form a stable helix is 12 hence the oligomeric arms attached to the chromophore cannot form a helix on their own. Moreover, the communication between the two oligomeric arms of one chromophore is not possible because of the linear structure of the *trans*-azobenzene. However, photoisomerization should result in a curved structure of *cis*-azobenzene. This curvature should allow the communication between the two oligomeric arms via π,π–stacking interactions among the neighboring aromatic repeat units. Thereby, stable helices of 12 and 20 repeats units are expected to be formed from oligomers **11** and **12** by irradiation in a helix-promoting solvent.

Synthesis of the Oligomers

Oligomers **2** and **3** were prepared from commercially available methyl 3-nitrobenzoate in twelve and fifteen synthetic steps respectively. Methyl 3-nitrobenzoate was brominated and reduced followed by triazene formation and transesterification, finally palladium-catalyzed coupling of trimethylsilylacetylene gave orthogonally protected monomer **1** (Scheme 1).

Scheme 1

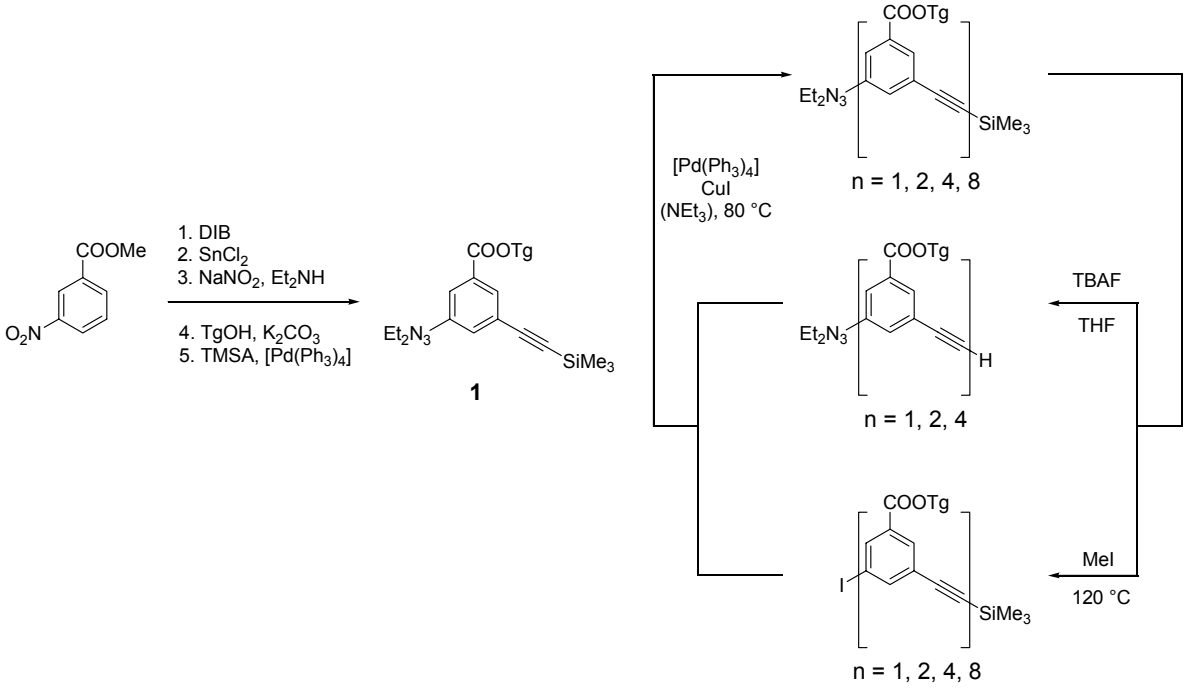

The terminal acetylene in monomer **1** is protected as a trimethylsilyl group, which can be removed by tetrabutylammonium fluoride and the triazene group can be converted to an iodine functionality by treatment with methyl iodode. This bifunctional orthogonally protected monomer is subsequently used to construct the higher oligomers. While one part of it was converted to free acetylene the remaining part was activated by transformation to a terminal iodide. Coupling of the free acetylene and iodide functionalities gave the orthogonally protected dimer. Tetramer and octamer were prepared in the same way. The end capper **4** was synthesized in 3 steps. Methyl 3-bromobenzoate was transesterified with triglyme monomethyl ether, followed by palladium-catalyzed coupling with trimethylsilylacetylene. Deprotection of trimethylsilyl group by tetrabutylammonium fluoride gave free acetylene **4,** which was coupled with oligomers **2** and **3** to yield the end capped oligomers **5** and **6**, respectively.

Scheme 2

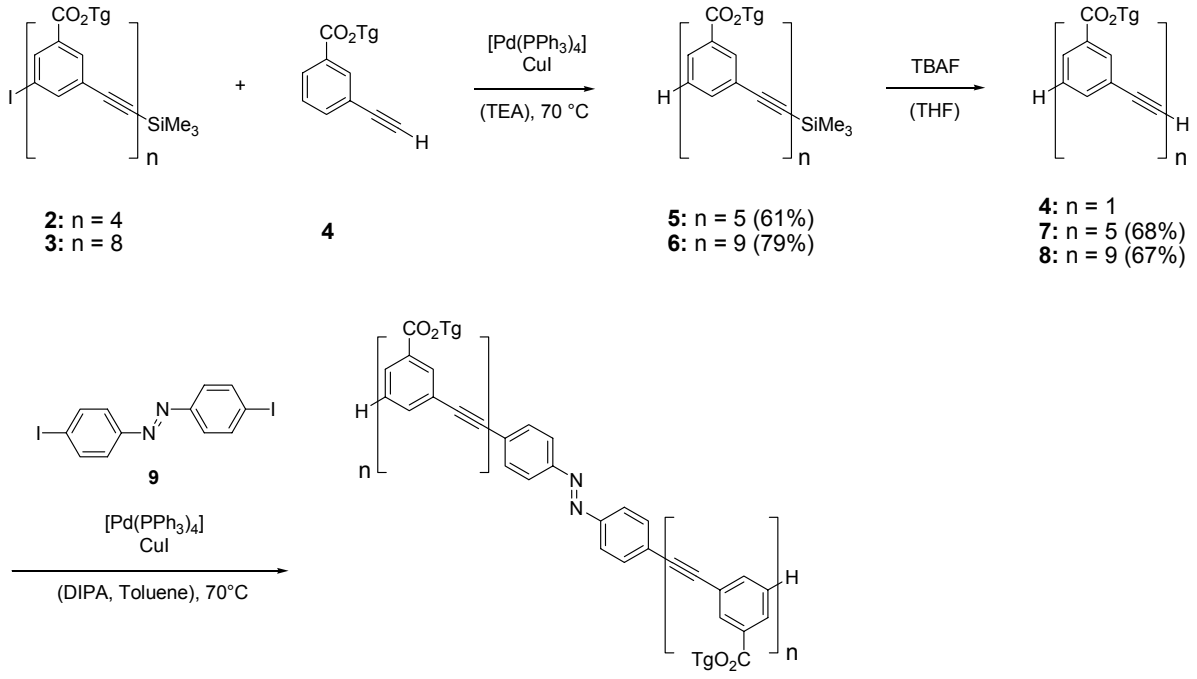

2: n = 4
3: n = 8

4

5: n = 5 (61%)
6: n = 9 (79%)

4: n = 1
7: n = 5 (68%)
8: n = 9 (67%)

10: n = 1 (65%)
11: n = 5 (30%)
12: n = 9 (46%)

The end-capping of oligomers is important as the terminal iodide group potentially interferes with the fluorescence measurements by emission quenching. The trimethylsilyl groups of oligomer **5** and **6** were deprotected followed by palladium-catalyzed coupling of azo-diiodide **9** to give oligomers **11** and **12** (Scheme 2). The model compound was synthesized by coupling of

free acetylene **4** with the azo-diiodide **9** (Scheme 2)**.** These oligomers were thoroughly characterized by several analytical tools. For example, ^{1}H NMR spectroscopy permitted rapid identification of the molecular structure where the presence of only one set of end group protons is indicative of a symmetrical structure, provide a convenient measure of the oligomer length. MALDI-TOF mass spectrometry measurements corroborated the NMR results by showing the expected $[M + Na]^{+}$ signal. Each oligomer exhibited a single, symmetrical peak in gel permeation chromatograms. The purities of these oligomers were determined to be greater than 99% based on GPC (Figure 4).

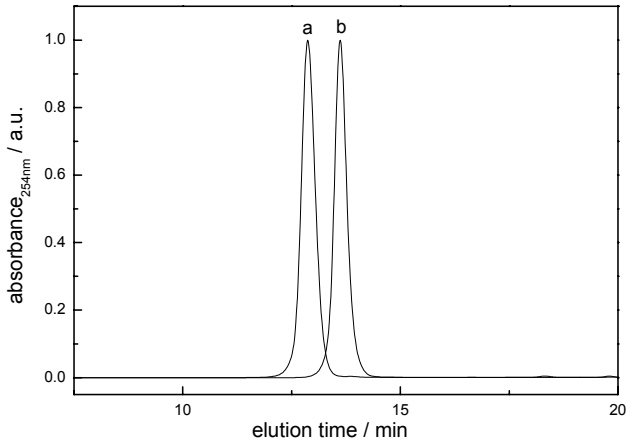

Figure 4. Gel permeation chromatograms of oligomers **11** (a) and **12** (b) in THF. Both traces have been normalized to a maximum intensity of 1.0.

Photoisomerization Studies

In order to study the photoresponsive behavior, of oligomers 10-12, absorption spectra were recorded in chloroform and acetonitrile (Figure 5). Compound **10** having monomeric appended strand segments (n = 1) was used as a model compound for the initial studies on photoisomerization of the azobenzene chromophore. Only one absorption maximum can be seen at 381 nm corresponding to the $\pi-\pi*$ transition of the *trans*-isomer of the extended azobenzene chromophore.

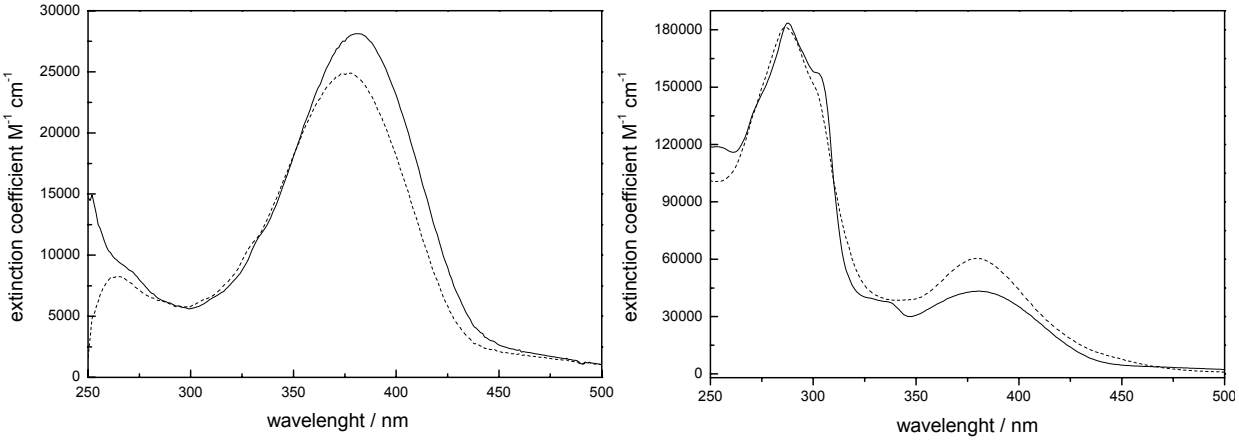

Figure 5. UV-visible absorption spectra of oligomer **10** (left) in $CHCl_3$ (——) and CH_3CN (— —) and oligomer **11** (right) in $CHCl_3$ (——) and CH_3CN (— —) (25 °C).

The strong bathochromic shift of the azobenzene core in oligomers **10-12** as compared to the native chromophore (λ ~ 320 nm) is a result of the extended π–conjugation due to *para*-substitution with the phenylacetylene unit. Upon irradiation at 395 nm, the low energy absorption spectrum shows an increasing yet weak band at 480 nm attributed to the lowest singlet state of the n-π* character. Where the intensity of this band is almost negligible for the *trans*-isomer due to a symmetry forbidden transition, the transition becomes weakly allowed when the molecule is distorted in its *cis*-form. The second band at 381 nm belonging to the π–π* transition of the *trans*-isomer gradually depletes with increasing exposure time and a new band starts to appear at 289 nm. This band belongs to the π–π* transition of the *cis*-isomer. The marked difference of π–π* transition of the two isomers can be explained by the non-planer conformation and hence loss of conjugation in the *cis*-isomer. Two clear isosbestic points can be detected at 335 and 449 nm confirming clean interconversion between two species. The photostationary state is reached after an irradiation time of 2 min. In the dark at room temperature the photogenerated *cis*-form slowly reverts back to the *trans*-form in the dark confirming the reversibility of the isomerization (Figure 6).

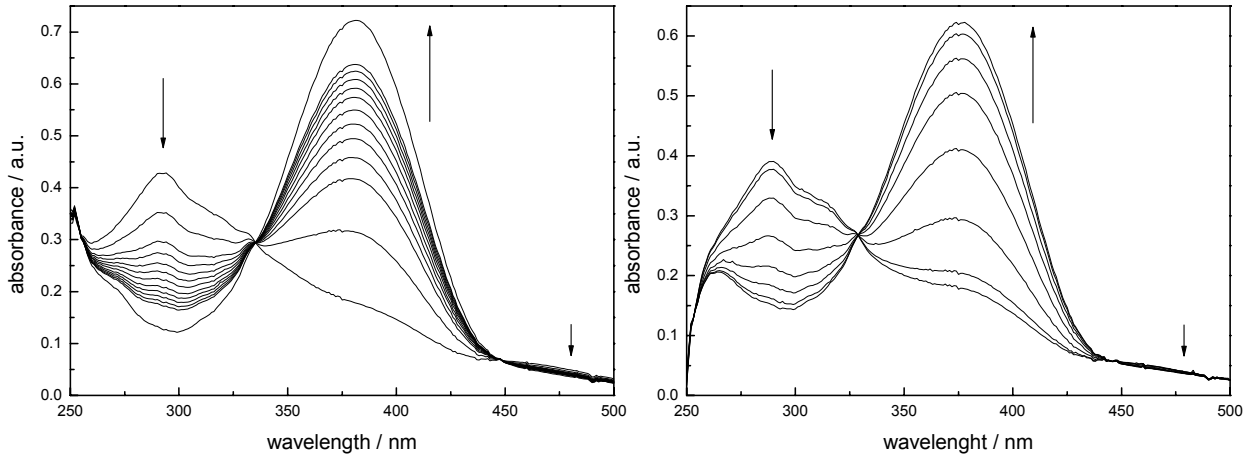

Figure 6. UV-visible absorption spectra of oligomer **10** in $CHCl_3$ (left) and CH_3CN (right) showing thermal relaxation at 25 °C after irradiation at 395 nm.

Figure 7 shows the thermal *cis*→*trans* isomerization of oligomer **11** in chloroform and acetonitrile after irradiating at 395 nm for 2 min. The absorption maximum at 290 nm is due to the phenylene ethynylene backbone, while the band centered at 395 nm is due to the azobenzene core. Irradiation causes an increase in the absorption in the range of the backbone chromophore at 290 nm. This is related to the contribution of the *cis*-isomer of the azobenzene core to this absorption band. Two well-developed isosbestic points can be detected at 339 and 448 nm.

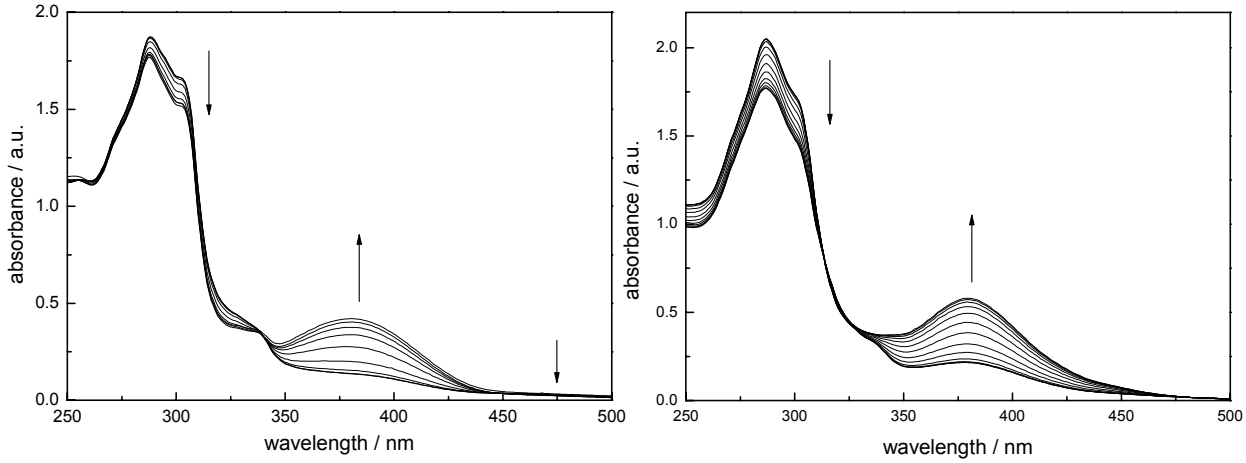

Figure 7. UV-visible absorption spectra of oligomer **11** in $CHCl_3$ (left) and CH_3CN (right) showing thermal relaxation at 25 °C after irradiation at 395 nm.

In addition, the longest oligomer i.e. **12** was also exposed to 395 nm light for 2 min. Figure 8 shows the thermal *cis→trans* isomerization of oligomer **12**. The same features can be seen as in the case of oligomer **11,** with two clear isosbestic points at 339 and 448 nm, yet the backbone absorption obviously dominates the overall spectrum.

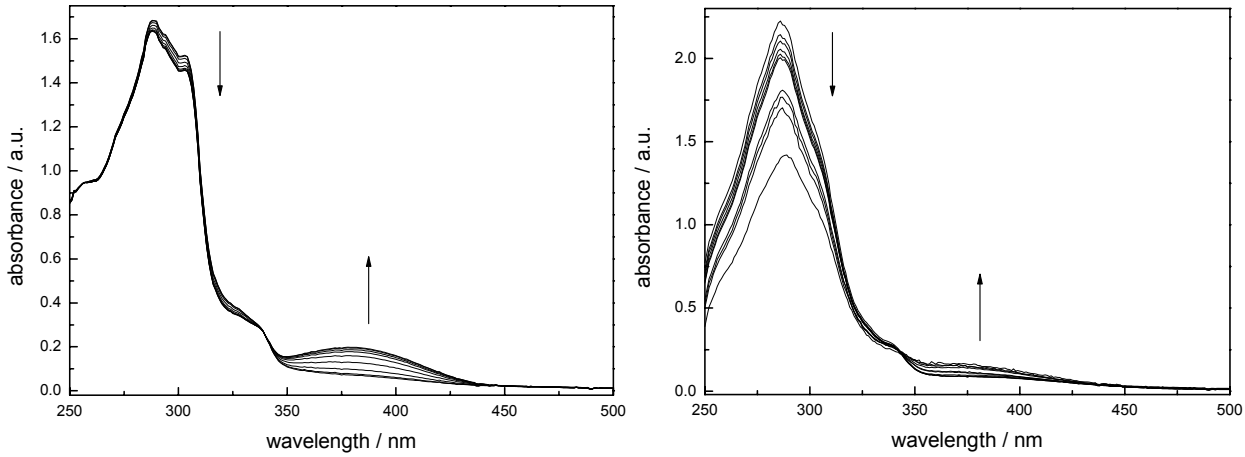

Figure 8. UV-visible absorption spectra of oligomer **12** in $CHCl_3$ (left) and CH_3CN (right) showing thermal relaxation at 25 °C after irradiation at 395 nm.

Thermal cis→trans isomerization

Due to the anticipated conformational change accompanying both photochemical and thermal isomerization, we were interested in studying the kinetics to reveal potential affects on the rates of interconversion. In view of the convenient time frame of the thermal *cis→trans* isomerizationhaving half-lives on the order of hours, thermal reversal of solutions in the photostationary state was investigated as a function of chain length and solvent (the temperature was kept constant at 25 °C). For example, the rate of *cis→trans* isomerization of oligomer **10** should be similar in two different solvents as it is too short to form a helix, where as in oligomers **11** and **12,** if forming helical conformation upon isomerization should have a slower back reaction in the helix promoting solvent as favorable π,π–stacking interactions have to be broken in order to reach the *trans*-resting state. The experimental results (Table 1) reveals that the rates are strongly dependent on solvent yet *no chain length dependence* as anticipated by helical folding, was found.

Table 1 Rates of thermal beck reaction for oligomers **10**, **11,** and **12** in chloroform and acetonitrile

Oligomer	k_{rev} in chloroform	k_{rev} in acetonitrile
10 (n = 1)	$k = 7.89 \pm 0.04\ 10^{-5}\ s^{-1}$	$k = 3.51 \pm 0.05\ 10^{-5}\ s^{-1}$
11 (n = 5)	$k = 8.90 \pm 0.08\ 10^{-5}\ s^{-1}$	$k = 1.26 \pm 0.09\ 10^{-5}\ s^{-1}$
12 (n = 9)	$k = 9.09 \pm 0.47\ 10^{-5}\ s^{-1}$	$k = 1.62 \pm 0.19\ 10^{-5}\ s^{-1}$

Fluorescence Spectroscopy

Fluorescence spectroscopy is a valuable tool to study conformational changes of oligo(*m*-phenylene ethynylene)s foldamers. In denaturing solvents such as chloroform, emission from individual non-communicating repeat units is observed, due to the absence of a specific conformation while in polar solvents, such as acetonitrile, the helical conformation prevails and hence excimer-like emission arising from the π–stacked aromatic rings is seen (see also Chapter 1). The fluorescence spectra of oligomer **11** shows (Figure 9) band at 350 nm before and after irradiation in chloroform. In acetonitrile, the presence of a helical secondary structure is unlikely before irradiation because the attached oligomers on both sides of the azobenzene core are not long enough to fold into individual helices. Hence, the monomer emission can be seen in acetonitrile before irradiation. However, irradiation at 395 nm in acetonitrile causes *no change* in the emission spectra (except low intensity) suggesting that there is no conformational change associated with the photoisomerization.

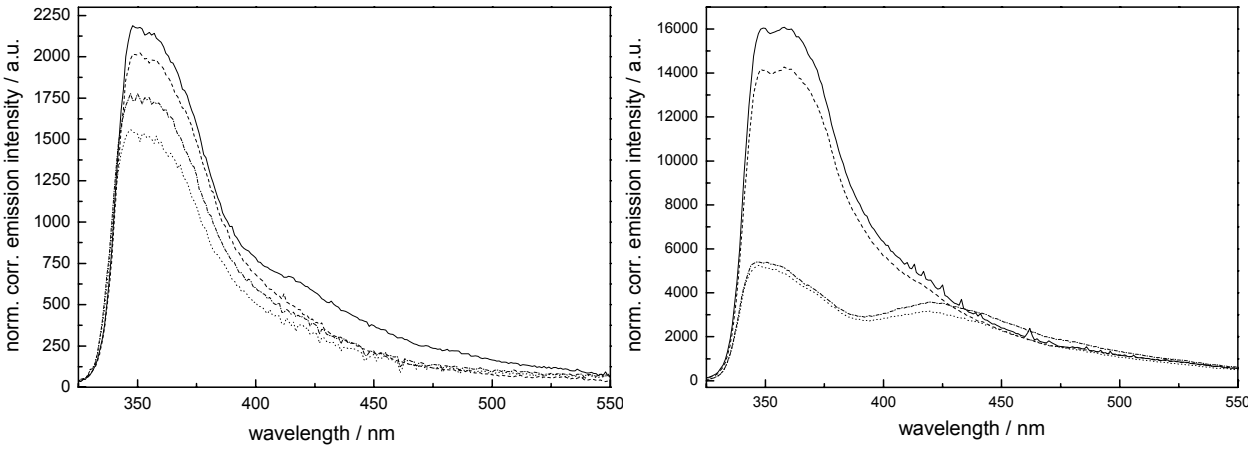

Figure 9. Fluorescence spectra of oligomer **11** (left), before irradiation (— —), after irradiation (——) in $CHCl_3$ and before irradiation (·····), after irradiation (— · —) in CH_3CN, and oligomer **12** (right), before irradiation (— —), after irradiation (——) in $CHCl_3$ and before irradiation (·····), after irradiation (— · —) in CH_3CN using an excitation wavelength of 290 nm (25 ^oC).

In the case of longer oligomer **12** Chloroform solution, before and after irradiation show the expected monomer emission at 350 nm. In acetonitrile, however, before irradiation the 350 nm band shows unexpected partial quenching of monomer emission and appearance of a red shifted, broad featureless band centered at 425 nm. This band can be attributed to the π–stacked aromatic chromophores and indicates that there is some population of folded oligomers in solution before irradiation. Most likely the electron-deficient azobenzene core engages in stronger π,π–stacking interactions leading to more pronounced stabilization of the helical conformation and hence folding at shorter lengths as compared to the native *meta*-linked phenylene ethynylene oligomers.[17] The same band is observed after *trans-cis* photoisomerization indicating that there is no significant conformational change in the folding backbone before and after irradiation. The non-planarity of *cis*-azobenzene perhaps destabilizes the helical conformation by disturbing the π,π–stacking interactions and hence prevents formation of a stable helix.

Turn-off helices

We anticipated that *meta*-substituted *tans*-azobenzene would structurally compliment a single unit of diphenylacetylene in Oligo(*m*-phenylene ethynylene)s foldamer. The *trans*-state of the chromophore should provide the necessary curvature in the structure to form a helix in polar

solvents while irradiation should result in disruption of the helical conformation by breaking the aromatic contacts due to the non-planarity of the *cis*-azobenzene (Figure 10).

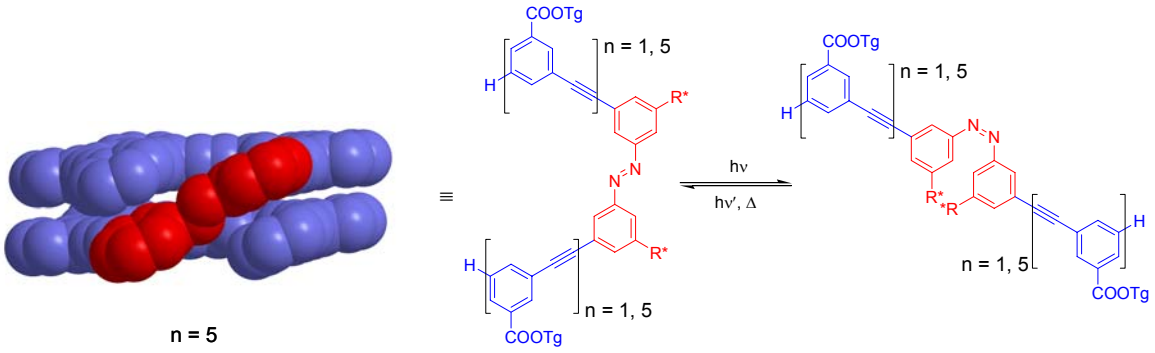

Figure 10. Photoisomerization of oligo(*m*-phenylene ethynylene)s foldamer containing a *meta*- substituted azobenzene core (Right). A space filling model showing the proposed helical conformation of oligomer **18** in the *trans*-azobenzene resting state.

Synthesis of the Oligomers

The synthesis of the azobenzene core molecule **16** was accomplished in 3 steps. Methyl 3-nitrobenzoate was brominated followed by treatment with zinc under basic conditions to give the desired bis-acid **14**. The bis-acid was converted to the corresponding acid chloride in refluxing thionyl chloride. The acid chloride was used without further purification and esterified with the chiral alcohol **15** to give azobenzene core **16**.

Scheme 3

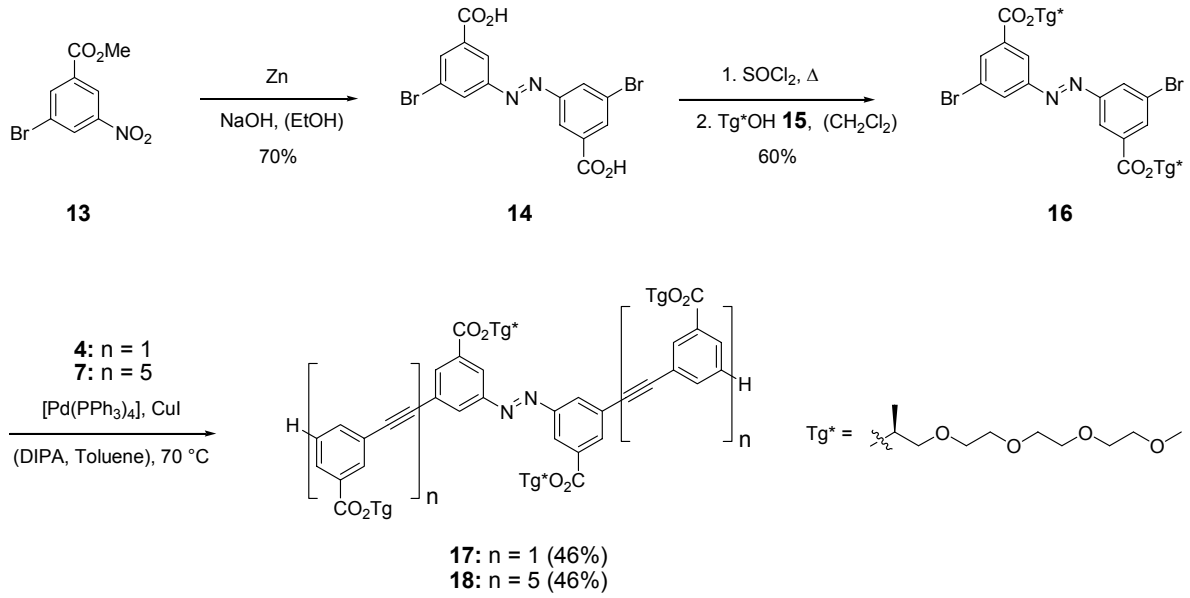

The introduction of chiral alcohol **15** was deliberate so as to study the conformational changes of the oligomer with the help of CD spectroscopy. The bis-bromide **16** was coupled to oligomer **4** and **7** by palladium-catalyzed coupling to yield model compound **17** and oligomer **18**, respectively (Scheme 3). The structural integrity and purity of these oligomers were verified by several analytical tools, including ^{1}H NMR, MALDI-TOF MS and GPC (Figure 11).

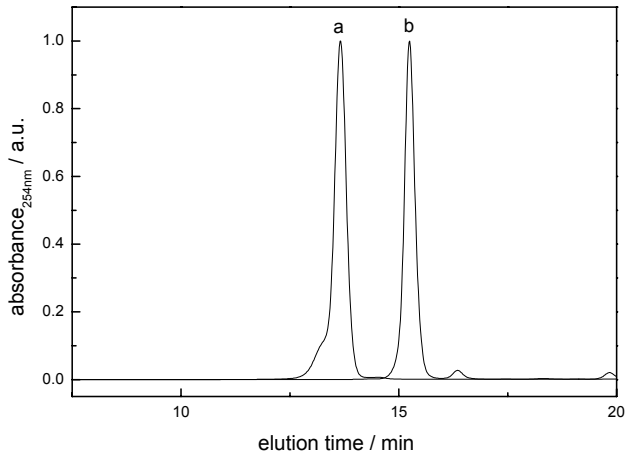

Figure 11. Gel permeation chromatograms of oligomers **17** (a) and **18** (b).in THF. Both traces have been normalized to a maximum intensity of 1.0.

Folding Studies in the Dark State

The absorption spectrum of the phenylacetylene chromophore shows two absorption maxima at 288 and 303 nm. These two peaks can be regarded as two vibronic bands belonging to the *cisoid*- and *transoid*- conformation of the phenylene ethynylene backbone (Chapter 1). The conformational change of the oligo(*m*-phenylene ethynylene)s results in hypochromism of 303 nm band. Figure 12 shows the absorption spectrum of model compound **17** and oligomer **18**. In chloroform the absorption spectra of **18** exhibit two typical bands at 288 and 309 nm. This indicates that the oligomer exist as a random coil.

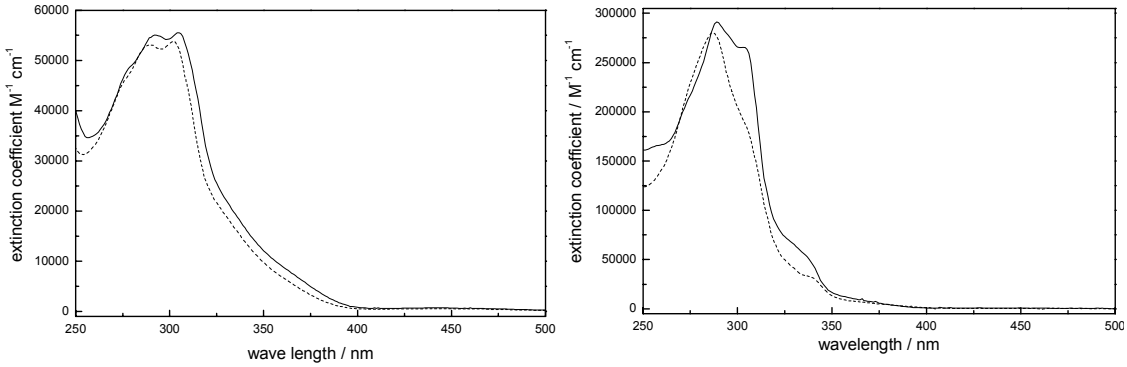

Figure 12. UV-visible spectra of oligomer **17** (left) in $CHCl_3$ (——) and CH_3CN (— —) and oligomer **18** (right) in $CHCl_3$ (——) and CH_3CN (— —) (25 ^oC).

In a typical solvent denaturation experiment addition of acetonitrile causes a decrease of the 303 nm band and in pure acetonitrile this band vanishes completely. The absorbance ratio (A_{303nm}/A_{288nm}) furnished a value of 0.65. Smaller ratios (A_{303nm}/A_{288nm}) relates to a large decrease in the 303 nm band belonging to the *transoid*-state and implies that a high number of molecules adopt helical conformation. The titration curve is represented by plotting (A_{303nm}/A_{288nm}) vs solvent composition and reveals a sigmoidal shape indicative of the cooperative folding process (Figure 13).

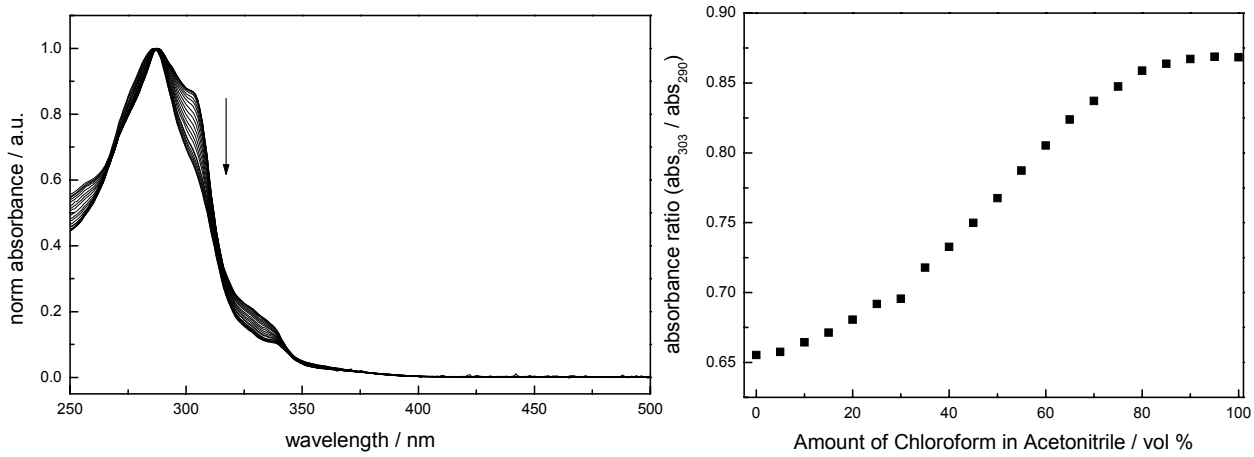

Figure 13. UV-visible absorption spectra of oligomer **18** in $CHCl_3$ (left) with increasing CH_3CN content (100% $CHCl_3$ → 100% CH_3CN). The spectra, measured at approximately the same concentration, have been normalized with respect to their maximum intensity. Plot of the UV-vis absorbance ratio (A_{303nm}/A_{290nm}) as a function of the volume percent chloroform in acetonitrile (right) (25 °C).

The lower left part of the curve with low absorbance ratios represents pre-transition period where all the molecules are in folded helical conformation. The upper right part of the curve with high absorbance ratios shows the post-transition state, here the solvent mixture contains mostly denaturing solvent and therefore a large number of molecules exist in random coil conformation. These two plateaus are connected by the region of the folding transition. The sharp nature of the transition furthermore supports cooperative nature of the folding event. Using solvent denaturation data, the helix stabilization energy in pure acetonitrile $\Delta G(CH_3CN)$ was calculated to be -1.6 kcal/mol. While these results already show the folding of oligomer **18,** fluorescence spectroscopy did not aid conformational analysis (Figure 14).

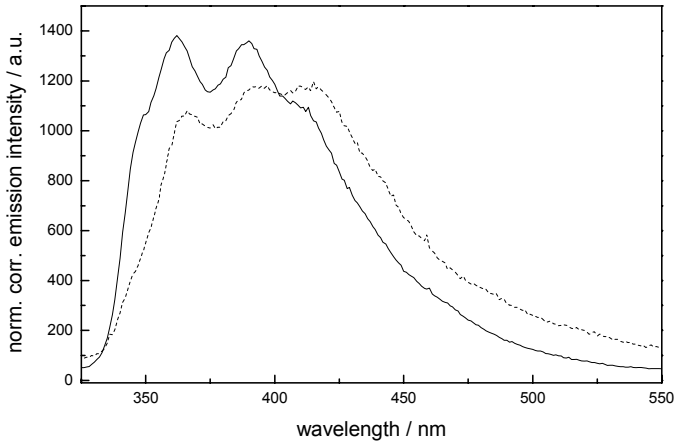

Figure 14. Fluorescence spectra of oligomer **18** in $CHCl_3$ (——) and CH_3CN (— —) using an excitation wavelength of 290 nm (25 ^oC).

To gain additional insight into the prevailing solution conformation CD spectroscopy was employed to study oligomer **18** that was decorated with two chiral interior side chains. This technique measuring excess chirality, e.g. helicity, is widely used to determine the secondary structure of naturally occurring biomacromolecules. In order to generate excess helicity, the twist sense of the otherwise racemic and hence CD-inactive mixture has to be biased, for instance by introduction of chiral groups. Incorporation of enantiomerically pure chiral side chains results in the formation of distereoisomeric helices with different energy and hence non-equivalent ratio.

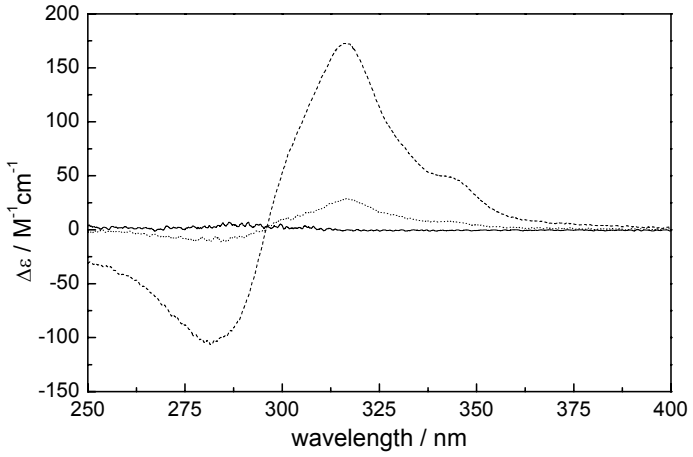

Figure 15. CD spectra of oligomer **18** in chloroform (——), acetonitrile (·····) and 40 vol% water in acetonitrile (25 °C).

As expected oligomer **18** shows no CD signal in chloroform as there is no secondary structure present in the solution. In acetonitrile, however, oligomer **18** adopts a helical conformation as evident by UV-vis spectroscopy and hence a CD signal can be seen in the back bone absorption region (250-350 nm). However, this signal is very weak and suggests that the energy difference, separating both of distereoisomeric helices, caused by the chiral side chains is not large enough to strongly shift the equilibrium. The helix twist sense can further be biased by addition of water to acetonitrile. This makes the environment more polar and increases the solvophobic interactions and as a result, a more intense CD signal can be seen (Figure 15). The shape of the CD-spectrum indicates P-helicity. Interestingly, side chains having β-methyl instead of α-methyl substitution, show inverse helicity. [18]

Irradiation studies

The photoisomerization of oligomers **17** and **18** were unsuccessful as irradiation at 320 nm resulted in irreversible changes in the absorption spectra (Figure 16).

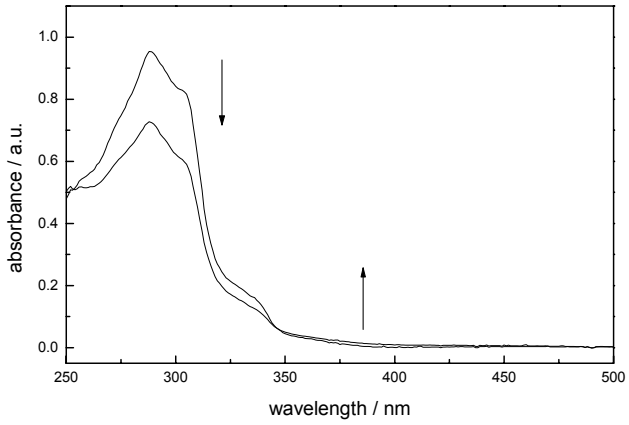

Figure 16. Irreversible changes in the UV-visible absorption spectra of oligomer **18** (left) in $CHCl_3$ using an excitation wavelength of 320 nm (25 ^{o}C).

This behavior can be understood in the following way. In case of oligomers **11** and **12** the azobenzene chromophore was in conjugation with one unit of phenyl acetylene on both sides, the absorption band of the photochromic molecule was centered at 390 nm, the lack of conjugation in the case of oligomer **17** and **18** due to *meta*-connectivity leads to a blue-shifted absorption centered at 320 nm. Since At this wavelength the backbone absorbs quite strongly, as illustrated by the absorption coefficients (Figure 12) selective excitation of the azobenzene is not possible and the light is mainly absorbed by the backbone leading to yet unidentified irreversible photochemistry.

Selective excitation of azobenzene chromophore

To excite azobenzene chromophore selectively it is necessary to avoid the overlap between the two bands arising from the backbone chromophore and the azobenzene chromophore. To solve this problem one can use the donor acceptor substituted azobenzene chromophores, which are known to absorb at rather long wavelength but the short life time of their *cis*-form could be a limitation to our studies. the conformational changes carefully. The other way is to provide two donor substituents to the azobenzene chromophore. If an azobenzene is substituted with an electron-donating group at its *para*- position, the first $\pi-\pi*$ transition will be of lower energy than in the unsubstituted azobenzene and hence this substituent effect is expected to cause bathochromic shift in the absorption spectrum. Due to the synthetic reasons, we chose *para*- substitution of the azobenzene by a methoxy. Figure 17 shows the absorption spectra

of compound **16** with absorption maxima at 320 nm and its methoxy-substituted analogue **24** having an absorption maximum at 350 nm. This clearly demonstrates that the absorption band of azobenzene chromophore can be shifted by 30 nm when electron-donating groups are in conjugation with the azobenzene chromophore and hence Selective excitation of the azobenzene core can now be achieved without interfering with the phenylene ethynylene backbone.

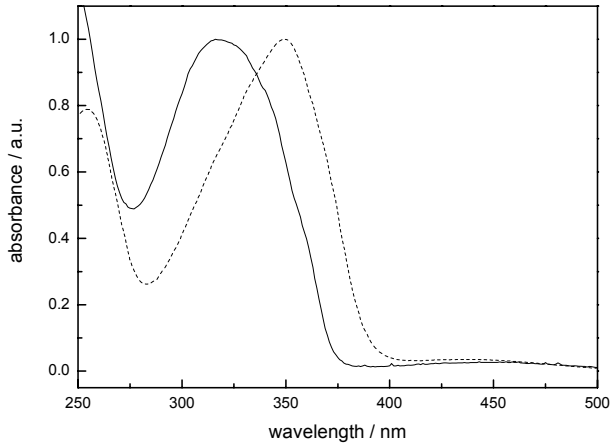

Figure 17. UV-visible absorption spectra of compound **16** (——) and **24** (·····) in chloroform (25 ^{o}C).

Synthesis of Donor-Substituted Azobenzene-core Foldamer

The synthesis of methoxy substituted azobenzene core molecule **28** was accomplished in 9 linear synthetic steps. 5-Nitrosalicylic acid was methylated to give compound **19**. Attempts to synthesize the azobenzene by reductive coupling of two nitrobenzene moieties (scheme 4) failed and instead the debrominated compound was isolated. Hence the desired azobenzene molecule was accessed via an oxidative coupling of the corresponding aniline. Compound **19** was brominated and reduced to give aromatic amine **21**. The amine was oxidized to azobenzene molecule **22,** which was saponified to give bis-acid **23**. The bis-acid was converted to the corresponding bis-acid chloride with the help of thionyl chloride and esterified with the chiral alcohol **15** to give azobenzene core molecule **24**. The azobenzene core was extended by palladium-catalyzed coupling with trimethylsilylacetylene to give compound **25,** which was deprotected with tetrabutylammonium fluoride to give free acetylene **26**. The free acetylene **26** was treated with 10 fold excess of the diiodide **27** under Sonogashira-Hagihara coupling conditions at room temperature to avoid the oligomerization and polymerization side products.

The extension of azobenzene core **28** was deliberate. By this extension the dibromide functionality is converted to a diiodide functionality.

Scheme 4

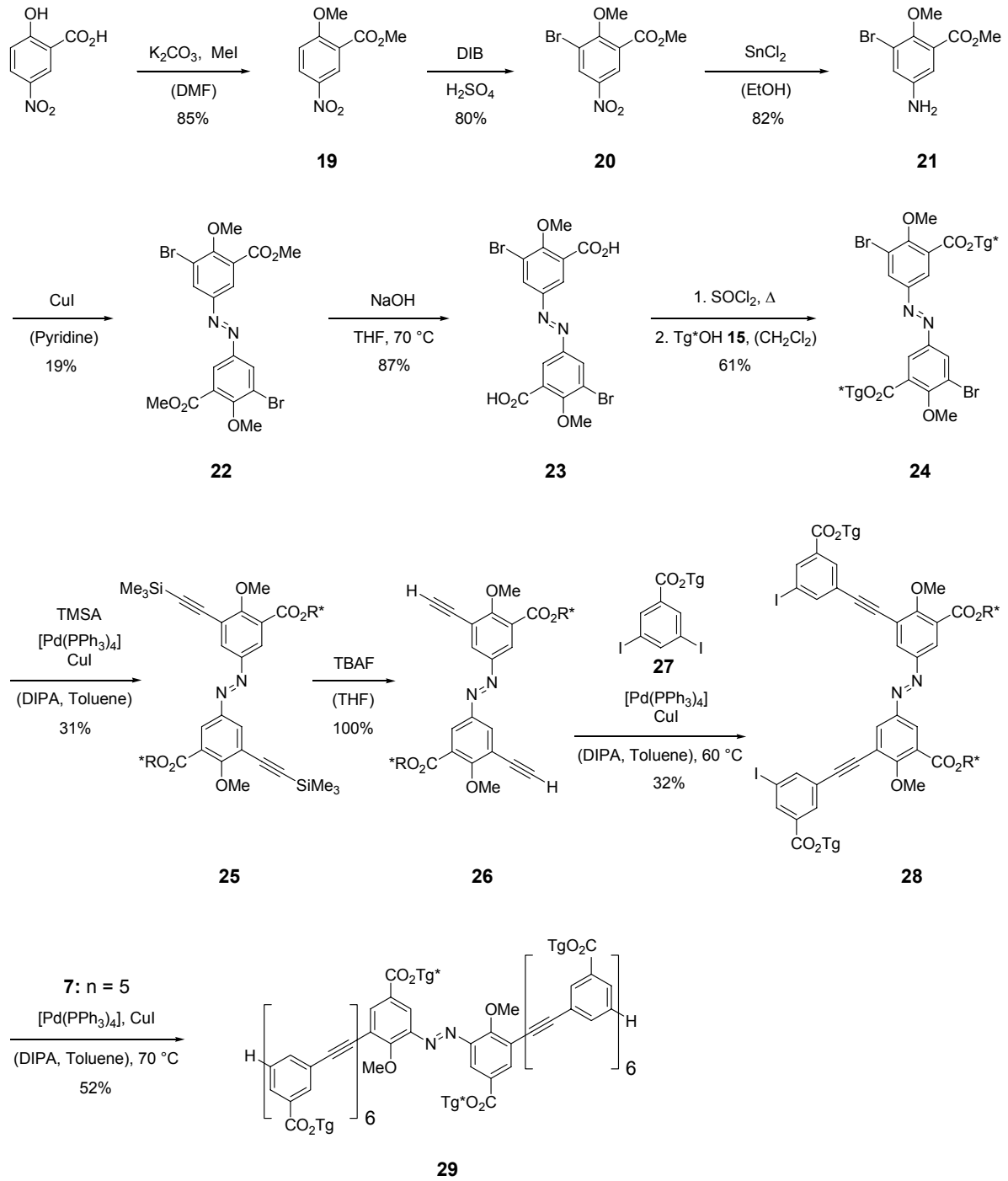

This is important due to the fact that we had limited access to pentamer acetylene **7** and use of dibromide **24** as coupling partner had severely limitations due to the low yielding coupling reactions presumably caused by more difficult oxidative addition to the *ortho*-methoxy substituted aryl bromide. The other more important fact was the synthesis of the oligomer with longer length was targeted as the improved analogue of **18** having two pentamer appended segments did not adopt a stable helical conformation in acetonitrile. Apparently introduction of the methoxy-groups significantly changes the electronics of the azobenzene moiety and consequently π,π–stacking interactions between the neighboring aromatic units are weakened.

The palladium-catalyzed coupling of diiodide **28** with free acetylene **7** gave the desired oligomer **29**. Several analytical tools such as ^{1}H NMR, ESI-MS, and GPC (Figure 18) were used to thoroughly characterize the oligomer **29**.

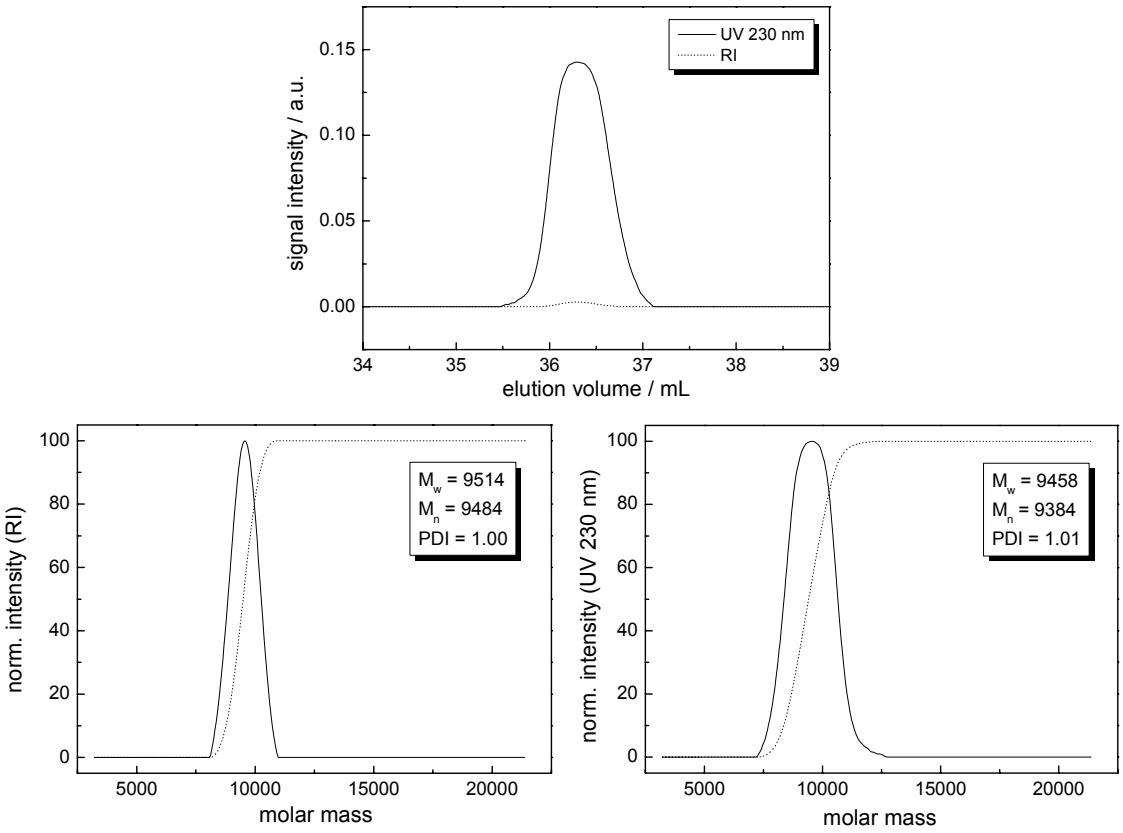

Figure 18. GPC chromatogram of oligomer **29** in THF (30 °C, polystyrene calibration**)**.

Photoisomerization Studies

Irradiation of the helically folded oligomer **29** using 365 nm light to selectively excite the central azobenzene chromophore led to rapid conversion to the corresponding *cis*-isomer as monitored by UV/vis absorption spectroscopy (Figure 19). The observed absorbance changes, i.e. decreasing π-π* (350–400 nm), weakly increasing n-π* (400–450 nm), and increasing π-π* (<265 nm) absorptions, as well as the presence of two well-defined isobestic points at 265 nm and 418 nm are indicative of the *trans*→*cis* photoisomerization process.[2] While the photochemical *trans*→*cis* conversion is achieved within seconds of irradiation time, the thermal *cis*→*trans* reversion occurs over the time frame of several hours at room temperature.

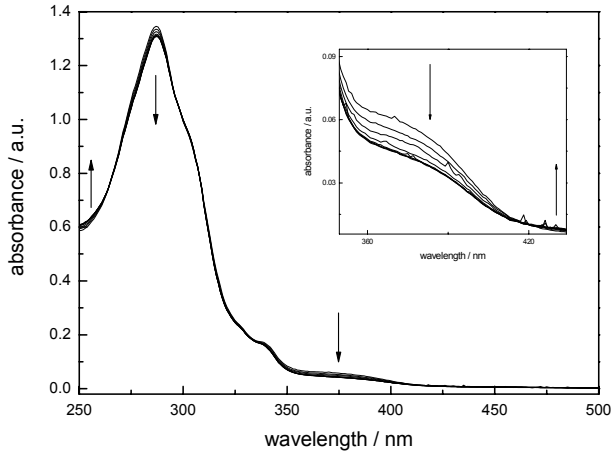

Figure 19. UV-vis absorption spectra spectra obtained during photochemical *trans-cis* isomerization of oligomer **29** caused by 365 nm irradiation in acetonitrile at 25 °C (t = 0, 1, 3, 7, 15, 31, 63 s). The inset shows a magnification of the characteristic π–π∗ band of the azobenzene core.

Folding Studies in the Dark State

The folding behavior of azobenzene-core oligomer **29** was investigated by typical solvent denaturation experiments using UV/vis absorption to monitor the conformational equilibrium (Figure 20). The sigmoidal shape of the obtained titration curve is indicative of the cooperative folding process.

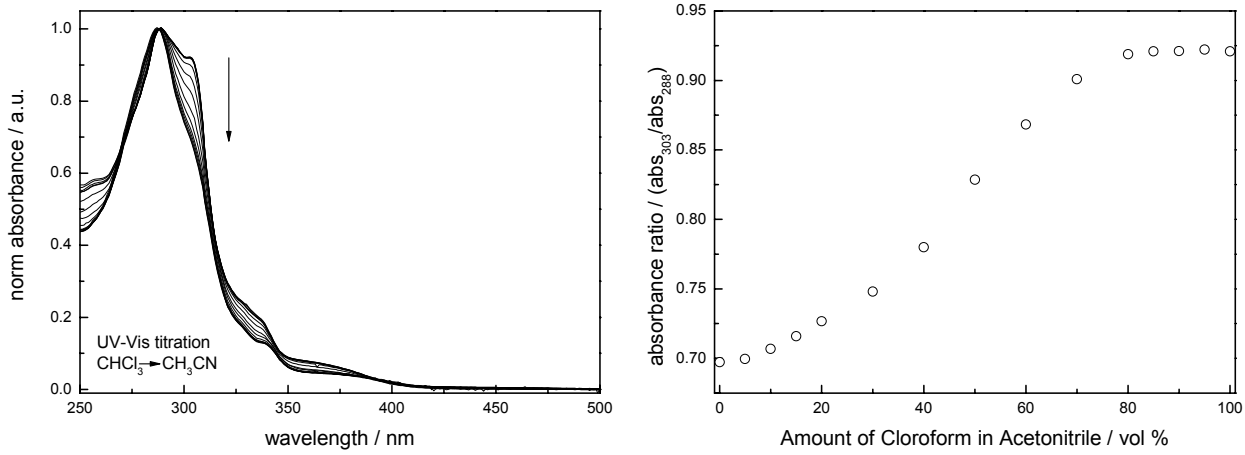

Figure 20. UV-visible absorption spectra of oligomer **29** in $CHCl_3$ (left) with increasing CH_3CN content (100% $CHCl_3$ → 100% CH_3CN). The spectra, measured at approximately the same concentration, have been normalized with respect to their maximum intensity. Plot of the UV-vis absorbance ratio (A_{303nm}/A_{290nm}) as a function of the volume percent chloroform in acetonitrile (right) (25 °C).

Detailed analysis of UV/vis data obtained in the titration experiments reveals a helix stabilization energy in pure acetonitrile $\Delta G(CH_3CN) = -1.7$ kcal/mol. Therefore, replacement of the central dimeric phenylene ethynylene unit in the native tetradecamer[10] by the azobenzene core leads to only slight helix destabilization that is attributed to weaker π,π-stacking interactions due to the presence of electron-donating methoxy-substituents.[17] (Figure 21).

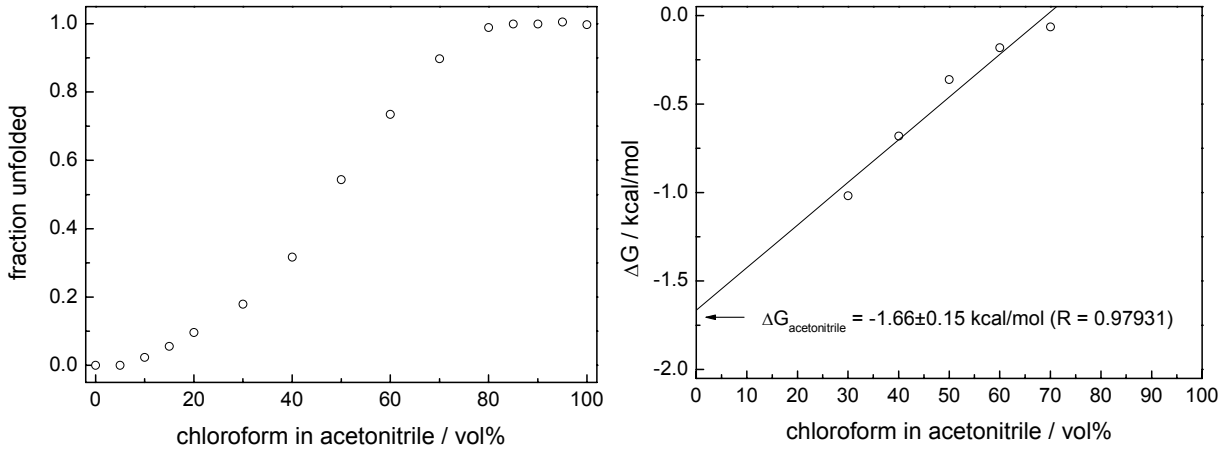

Figure 21. Normalized titration curve corresponding to UV/vis titration data shown in Figure 20 (left) and derivation of helix stabilization energy by linear regression of the data points in the transition region.

CD spectroscopy in pure acetonitrile did not reveal a large twist sense bias so again addition of water was investigated to increase the driving force for helical structure formation due to the solvophobic effect. In 60 vol% water in acetonitrile the induced CD signal is of significant intensity and proves the presence of the preferential *P*-helical conformation (Figure 22). These experiments compliment the evidence of helix formation by *trans*-azobenzene oligomer obtained by UV-vis spectroscopy.

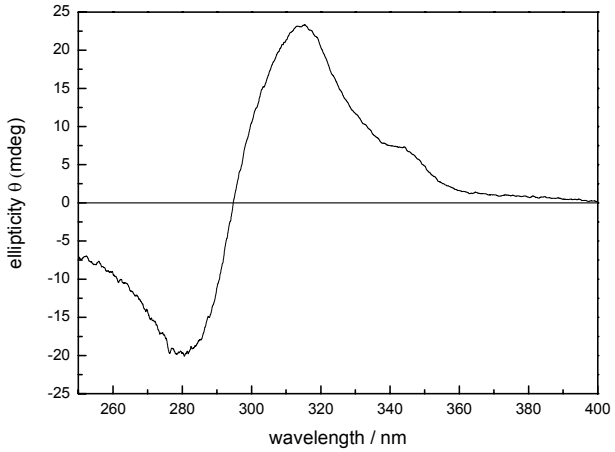

Figure 22. CD spectra of oligomer **29** recorded in 60 volume % water in acetonitrile. (25 °C)

Conformational Change during Photoisomerization as Monitored by CD

In order to monitor the conformational changes during both forward and backward isomerization processes, CD spectra of solutions of **1** in folding promoting solvent mixtures were recorded (Figure 23). The CD spectrum of **29** in aqueous acetonitrile shows a strong positive Cotton effect that can be assigned to the helical conformation, while in denaturing solvents, i.e. chloroform, no signal has been observed. The CD signal arises from exciton coupling within the helix and is the results of chirality transfer from the core's chiral side chains to the structure. Interestingly, the observed spectral shape indicating a (*P*)-helical twist sense is exactly opposite as compared to oligomers carrying side chains with the chiral methyl group in β-position.[18] While irradiation leads to a rapid decrease of the CD signal indicating depopulation of the helical conformation, i.e. unfolding, thermal reversion leads to a complete recovery of the initial CD signal intensity and therefore re-folding of the backbone. The presence of a well-developed isodichroic point at 295 nm suggests a clean conversion between both conformations. The composition of the mixture in the photostationary state (PSS) $\mathbf{29}_{cis}/\mathbf{29}_{trans} \sim 40\%$ can be directly

deduced from the ratio of the CD signals. Kinetic analysis of the data at 25 °C provides the rate of the thermal *cis→trans* isomerization $k_{cis\rightarrow trans} \sim 3.8 \cdot 10^{-5}\ s^{-1}$ corresponding to a half life $t_{1/2} \sim 5$ h and an activation energy $\Delta G^{\neq} \sim 23.5$ kcal/mol, typical for azobenzene-cored macromolecules in solution.[19]

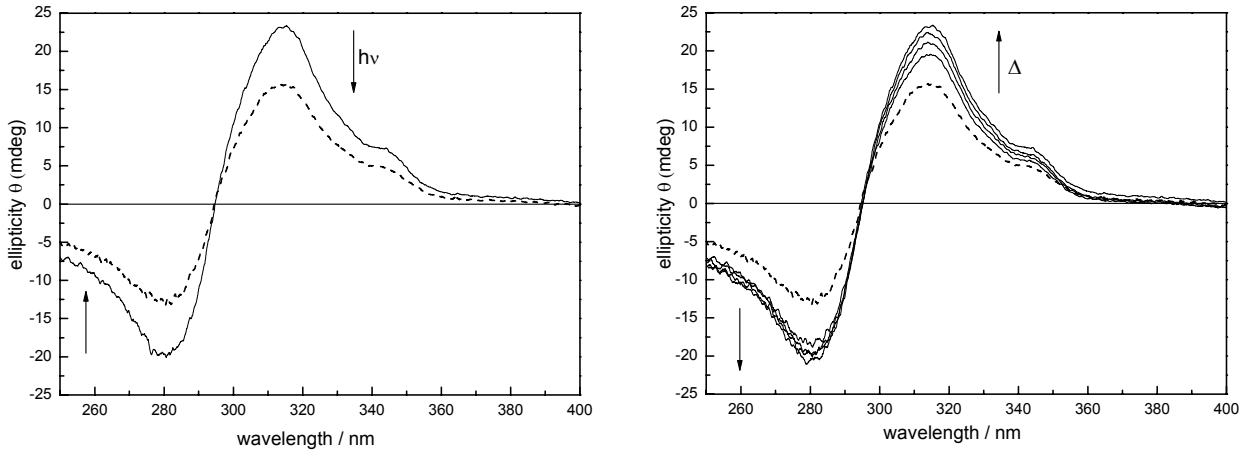

Figure 23. CD spectra of oligomer **29.** Before irradiation (——) and after irradiation (·····) at 365 nm (left). CD spectra recorded in the dark showing restore of the helical conformation due to thermal back relaxation of the azobenzene (Right). Spectra were recorded in 60 volume % water in acetonitrile at 25 °C.

Controlling the twist sense of a chiral foldamer

Achiral oligo (*m*-phenylene ethynylene) foldamer exist as a mixture of right- and left-handed helices interconverting dynamically in solution. This equilibrium between right- and left-handed helices can be biased in a number of ways. For example introduction of polar[20] and non-polar[21] chiral side chains, complexation of chiral guests[22], or incorporation of chiral cores.[23, 24] These structural changes results in distereoisomeric helices with one prevailing screw sense. However, no example has been reported, where this biased helix sense once formed due to primary structural changes, could be reversed.

We were interested in investigating the interaction between a chiral foldamer and a chiral guest. Oligomer **18** was chosen as host and (-) and (+)-α-pinene as host for these complexation studies (Figure 24).

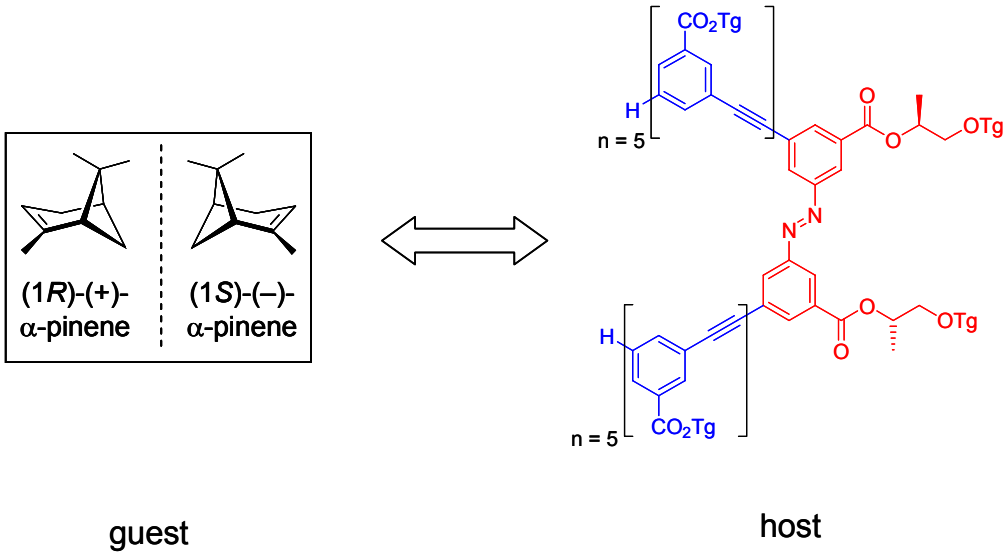

Figure 24. Structures of the pinene guest molecules (left) and chiral foldamer **18** (right) serving as host in complexation studies.

As shown before, pure acetonitrile does not give large distereomeric excess so different solvent compositions were investigated in order to search for the best conditions. Addition of water to acetonitrile constantly intensifies the CD signal (Figure 25). However, in 70 % aqueous acetonitrile the spectrum does not exhibit a well-defined isodichroic point any longer indicating that the oligomers are aggregating (into helical columns).[18] Hence, solutions containing, 40 vol % and 60 vol% aqueous acetonitrile were used for complexation studies.

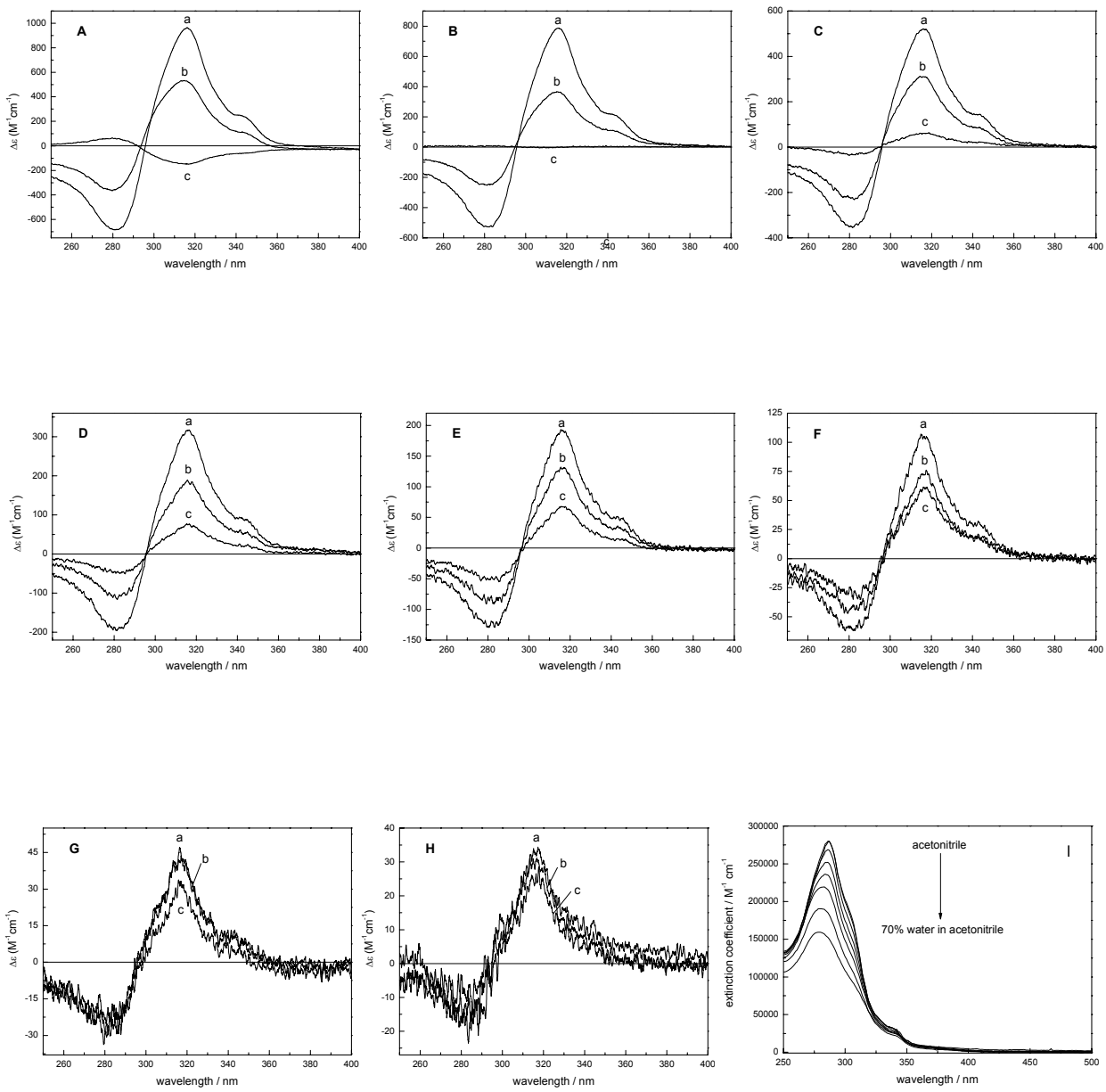

Figure 25. Complexation of oligomer **18** with (-) and (+) α pinene in different solvent compositions (volume % water in acetonitrile). Frame A- 70%, B- 60%, C- 50%, D- 40%, E- 30%, F- 20%, G- 10 % and H- 0%. Curve a) oligomer **18** with 150 equivalent (+) α pinene, b) oligomer **18** and c) oligomer **18** with 150 equivalent (-) α pinene (25 ^{o}C). The concentration of oligomer is always kept at 4.2 μM. Note the different ordinate scale. Frame I shows the absorption spectra of oligomer **18** in different solvent compositions.

Oligomer **18** as already demonstrated, exhibit a CD signal due to the presence of chiral side chains. The incremental addition of (+)-α-pinene to solution of oligomer **18** constantly enhances the CD signal gradually to saturation (Fig 26, 27).

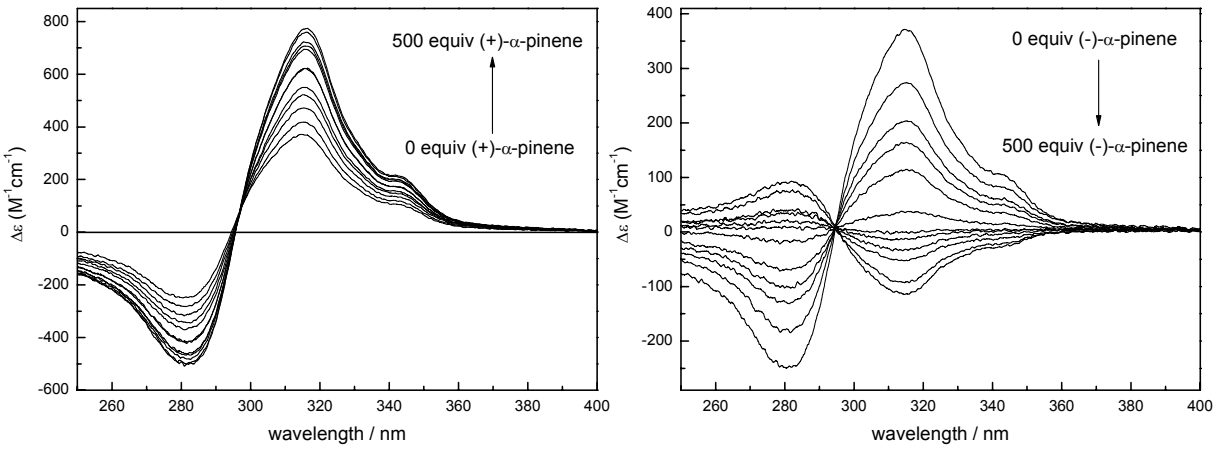

Figure 26. CD spectra of oligomer **18** as a function of (+) α pinene (left) and (-) α pinene (right) in 60 volume % of water in acetonitrile (25 ^{o}C). The concentration of oligomer is always kept at 5 μM. Note the different ordinate scale.

This means that the complexation of (+)-α-pinene within the tubular cavity of the chiral foldamer **18** act mutually with the chiral side chains to impart the same kind of handedness. (-)-α-pinene however competes with the chiral side chains in order to impart the opposite handedness to the helix. Incremental addition of (-)-α-pinene diminishes the CD signal and at higher (-)-α-pinene concentrations the sign of the CD signal actually starts to invert i.e. becomes negative. This indicates that at high (-)-α-pinene concentrations a majority of molecules reverse their helix sense. It can be seen from the Figure 26 and 27 that at higher water content smaller amounts of (-)-α-pinene are needed to reverse the helical twist sense.

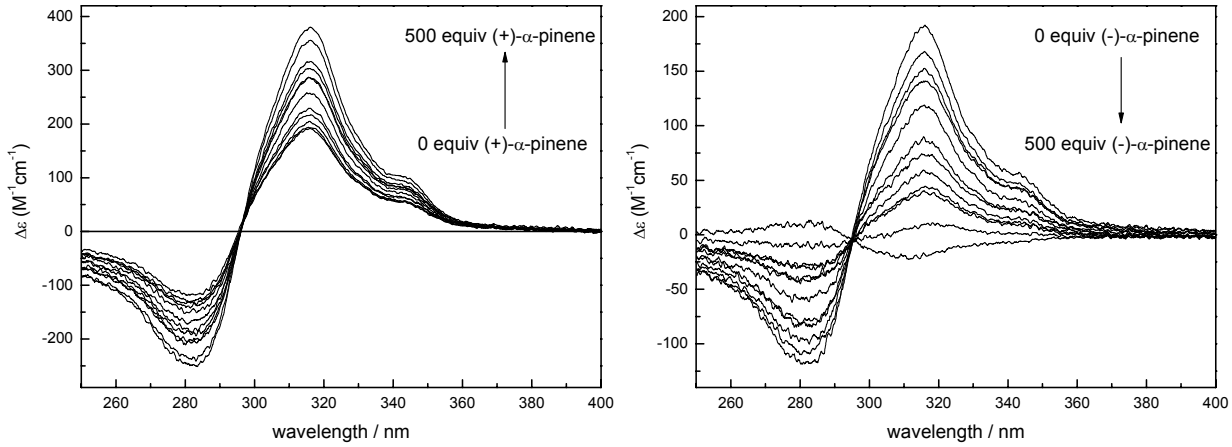

Figure 27. CD spectra of oligomer **18** as a function of (+) α pinene (left) and (-) α pinene (right) in 40 volume % of water in acetonitrile (25 ^{o}C). The concentration of oligomer is always kept at 5 μM. Note the different ordinate scale.

In folded oligomer **18** one lone pair of azobenzene nitrogen atom should be pointing towards the tubular cavity. Hence, we thought that this potential H-bond acceptor might associate strongly with guests presenting H-bond donors, i.e. alcohols. (+) and (-)-*trans* myrtanol and (+) and (-)-borneol were investigated with regard to their binding strength but as can be seen from Figure 28 they proved to be more weakly bound guests than α-pinene. A possible explanation for this observation is that the association of a non-polar guest, i.e. α-pinene, to the non-polar cavity of the foldamer is purely driven by solvophobicity while more polar alcohols i.e. guests myrtanol and borneol are better solubilized by the polar solvents and hence have a lower tendency to occupy the non-polar cavity of the foldamer host.

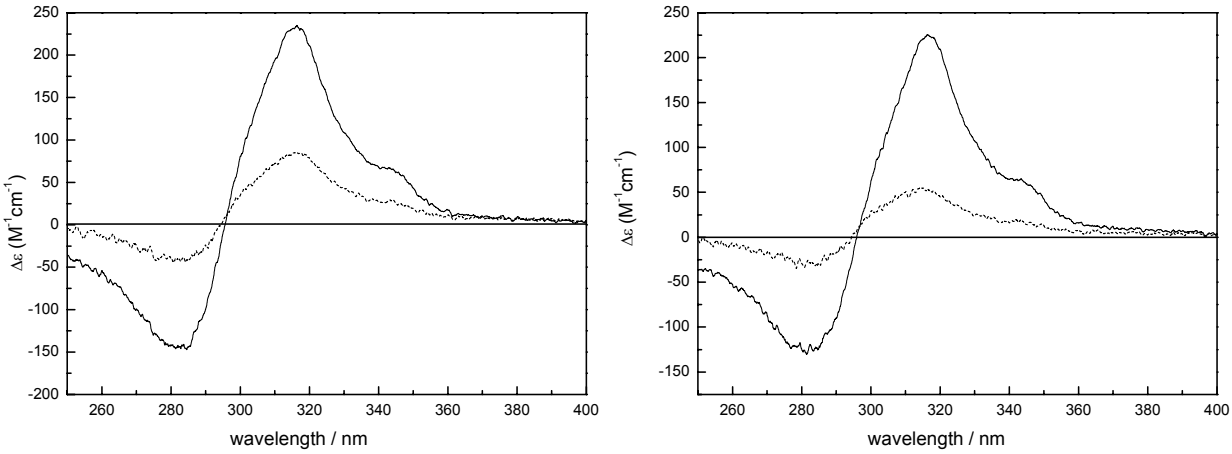

Figure 28. CD spectra of oligomer **18** with 500 equivalent (+) trans-myrtanol (——) and (-) trans-myrtanol (·····) (left) and 500 equivalent (+) borneol (——) and (-) borneol (·····) (Right).

Conclusion

We have demonstrated the feasibility of using light as an external stimulus to control the helix-coil transition in helically folding phenylene ethynylene oligomers after several design iterations. Introduction of a *meta*- connected *trans*-azobenzene chromophores in the backbone leads to formation of stable helices. These light-triggered systems can provide fundamental insight into the mechanisms of folding/unfolding by enabling time-resolved measurements and promise applications in photoresponsive materials and smart delivery devices based on photoresponsive dynamic receptors.

In-addition, specific interaction between small chiral guest and the chiral foldamer is shown to control the helix screw sense of these foldamers.

Experimental section

General Methods. Compounds **1**[25], **2**[11], **3**[11], **4**[11], **9**[26] **15**[27], **27**[28] were prepared as described in the literature. all other chemicals were commercial and used as received. THF and acetonitrile were distilled prior to use under N_2 atmosphere over sodium/benzophenone ketyl and calcium hydride, respectively. Column chromatography was carried out with 130-400 mesh silica gel. NMR spectra were recorded on Bruker AB 250 (250.1 and 62.9 MHz for ^1H and ^{13}C, respectively) and AC500 as well as Delta JEOL Eclipse 500 (500 and 126 MHz for ^1H and ^{13}C, respectively) spectrometers at 23 ± 2 ^oC using residual protonated solvent signal as internal standard (^1H: $\delta(CHCl_3)$ = 7.24 ppm, δ(DMSO) = 2.49, $\delta(CH_3CN)$ = 1.94 ppm and ^{13}C: $\delta(CHCl_3)$ = 77.0 ppm, δ(DMSO) = 39.7 ppm). Mass spectrometry was performed on Perkin-Elmer Varian Type MAT 771 and CH6 (EI), Type CH5DF (FAB), or Bruker Reflex with 337 nm laser excitation (MALDI-TOF) instruments. Elemental analyses were performed on a Perkin-Elmer EA 240. GPC measurements were performed on a Waters 515 HPLC pump-GPC system equipped with a Waters 2487 UV detector (254 nm detection wavelength) using THF as the mobile phase at 40 ^oC and a flow rate of 1 mL/min. The samples were separated through Waters Styragel HR1 or HR3 columns with 5 μm bead sizes. The columns were calibrated with several narrow polydispersity polystyrene samples and toluene served as internal standard.

Optical spectroscopy. UV/visible absorption and fluorescence emission spectra were recorded in various solvents of spectroscopic grade using quartz cuvettes of 1 cm path length on a Cary 50 Spectrophotometer and a Cary Eclipse Fluorescence Spectrophotometer, respectively, both equipped with Peltier thermostated cell holders (ΔT = ± 0.05 ^oC). Unless stated otherwise, all experiments were carried out at 25 ± 0.05 ^oC. For fluorescence measurements, the samples were not degassed since comparison of degassed with non-degassed solutions did not show measurable differences within the error of the experiment. The samples were excited at λ_{exc} = 290 nm, slit widths were set to 2.5 nm bandpass for excitation and 5 nm bandpass for emission. Fluorescence spectra were corrected for variations in photomultiplier response over wavelength using correction curves generated on the instrument. For titration experiments,[3] stock solutions in $CHCl_3$ and CH_3CN with optical densities OD(λ_{max}) ~ 0.8 for UV-visible absorption and OD(λ_{max}) ~ 0.1 for fluorescence measurements were used to prepare samples with varying solvent composition. The corrected fluorescence spectra were normalized by the exact OD_{289nm}. Circular dichroism spectra were recorded on a JASCO 700 spectrometer using quartz cuvetts of 1 cm path

length at 22 °C. In some cases circular dichroism Spectra recorded as θ in millidegrees, were converted to Δε using the equation $\Delta\varepsilon = \theta/(33982cl)$, where Δε is the difference in the molar absorptivity for oppositely polarized light in $M^{-1}cm^{-1}$, *c* is concentration in Mol/L, and *l* is the path length.

Irradiation experiments. Irradiation were performed using a LOT-Oriel 450-1000 W medium-pressure Xe lamp equipped with a water cooled liquid filter. For oligomers **10**, **11** and **12** the beam was passed through the water filter and then to a bandpass filter ($\lambda_{21\%T}$ = 395 nm). For oligomer **17** and **18** aqueous 0.17 M $NiSO_4$ solution filter ($\lambda_{28\%T}$ = 320 nm) was used. For oligomer **29** interference filter ($\lambda_{10\%T}$ = 365 nm) was used with following set up. A concentrated solution in acetonitrile was irradiated till photostationary state is reached. This solution was then diluted with water (60 volume %) and a CD spectra is recorded. This way is used because of easy detection of photostationary state in acetonitrile compare to acetonitrile water solvent mixture due to the hypochromicity of azobenzene in polar solvents. The solutions were degassed with argon for 5 min, before irradiation experiment.

Synthesis of the oligomers

Oligomer 5 (H-Ar$_5$-SiMe$_3$). Dry and degassed acetonitrile (12 mL) and triethylamine (20 mL) were added to a mixture of compound **4** (0.81 g, 2.8 mmol), **2** (4.0 g, 2.9 mmol), $Pd(PPh_3)_4$ (0.09 g, 0.08 mmol), CuI (0.2 g, 0.5 mmol), and PPh_3 (0.02 g, 0.05 mmol) the flask was sealed and heated to 70 °C for 16 hours. The reaction mixture was diluted with ethylacetate, filtered, concentrated and purified by column chromatography (1:4, acetone:chloroform) to give 2.6 g (61 % yield) of the product. ^{1}H-NMR (500 MHz, $CDCl_3$): δ 8.17-8.15 (m, 2 H, Ar-H), 8.12-8.10 (m, 6 H, Ar-H), 8.08-8.07 (m, 1 H, Ar-H), 8.03 (m, 1 H, Ar-H), 7.98-7.96 (m, 1 H, Ar-H), 7.83-7.80 (m, 2 H, Ar-H), 7.75-7.74 (m, 1H, Ar-H), 7.66-7.64 (m, 1 H, Ar-H), 7.40-7.37 (t, *J* = 7.7 Hz, 1H) 4.47-4.41 (m, 10 H, CO_2-CH_2), 3.80-3.76 (m, 10 H, O-CH_2), 3.66-3.56 (m, 30 H, O-CH_2), 3.46-3.43 (m, 10 H, O-CH_2), 3.27 (s, 3 H, O-CH_3), 3.26 (s, 9 H, O-CH_3), 3.26 (s, 3 H, O-CH_3), 0.19 (s, 9 H, Si-$(CH_3)_3$); ^{13}C NMR (500 MHz, $CDCl_3$); δ 164.79, 164.74, 138.59, 138.19, 135.65, 132.69, 132.54, 132.34, 132.26,130.92, 130.88, 130.67, 130.42, 128.41, 123.97, 123.73, 123.47, 123.44, 123.39, 123.34, 123.11, 122.81, 102.65, 96.34, 89.83, 88.97, 88.95, 88.87, 88.85, 88.78, 88.62. 88.09, 71.73, 70.50, 70.48, 70.46, 70.45, 70.42, 70.41, 70.40, 68.94, 68.88, 64.40, 64.17, 58.78, -0.36; FAB-MS (MNBA, 3 kV) *m/z* = 1525.6 (calcd 1526. for $C_{83}H_{101}O_{25}Si^+$).

oligomer 6 (H-Ar$_9$-SiMe$_3$). Free acetylene **4** (0.043 g, 0.15 mmol), oligomer **3** (0.374, 0.15 mmol), Pd (PPH_3)$_4$ (0.02 g, 0.02 mmol), CuI (0.002 g, 0.012 mmol) and PPh_3 (0.01g, 0.03 mmol) were suspended in triethylamine (6 mL) and the reaction mixture was heated at 70 °C for 15 hours. Removal of solvent followed by Column chromatography (1:3, Acetone:Cloroform) gave 0.21 g of the product as slightly pale white wax (79 % yield). ^{1}H NMR (500 MHz, $CDCl_3$, 23±2 ^{o}C): δ 8.21-8.19 (m, 2H, Ar-H), 8.18-8.16 (m, 12H, Ar-H), 8.15-8.14 (m, 1H, Ar-H -), 8.11 (m, 1H, Ar-H), 8.07 (m, 1H, Ar-H), 8.03-8.01 (m, 1H, Ar-H), 7.88-7.86 (m, 6H, Ar-H), 7.85-7.84 (m, 1H, Ar-H), 7.79-7.78 (m, 1H, Ar-H), 7.72-7.70 (m, 1H, Ar-H), 7.44 (dd, 1H, Ar-H J=7.7 Hz), 4.51-4.47 (m, 18H, CO_2-CH), 3.86-3.81 (m, 18H, O-CH), 3.71-3.68 (m, 18H, O-CH), 3.67-3.65 (m, 18H, O-CH), 3.63-3.61 (m, 18H, O-CH), 3.51-3.49 (m, 18H, O-CH), 3.33 (s, O-CH_3), 3.32(s, O-CH_3), 0.23 (s, 9H, Si-CH_3); ^{13}C NMR (125 MHz, $CDCl_3$): δ 164.99, 164.94, 138.36, 132.87, 132.79, 132.72, 131.08, 131.05, 123.60, 111.63, 92.09, 89.02, 71.89, 70.65, 70.63, 70.61, 70.57, 69.09, 64.58, 58.98, 48.54, 19.06, -0.21; (MALDI)-TOF MS (*trans*-indole acrylic acid matrix): *m/z* = 2708.06 (calcd 2708.08 for $C_{147}H_{172}O_{45}Si+Na^+$).

Oligomer 7 (H-Ar$_5$-H). Compound **5** (1.9 g, 1.3 mmol) was dissolved in 40 mL of THF and 2 mL of TBAF was added the reaction was stirred for a min and then filtered through silica gel and the crude mixture was purified by column chromatography (1:1, acetone:chloroform) to give 1.3 g (68 % yield) of the product. ^{1}H-NMR (500 MHz, $CDCl_3$): δ 8.17-8.15 (m, 2 H, Ar-H), 8.12-8.10 (m, 6 H, Ar-H), 8.08-8.07 (m, 1 H, Ar-H), 8.03 (m, 1 H, Ar-H), 7.98-7.96 (m, 1 H, Ar-H), 7.83-7.80 (m, 2 H, Ar-H), 7.75-7.74 (m, 1H, Ar-H), 7.66-7.64 (m, 1 H, Ar-H), 7.40-7.37 (t, *J* = 7.7 Hz, 1H) 4.47-4.41 (m, 10 H, CO_2-CH_2), 3.80-3.76 (m, 10 H, O-CH_2), 3.66-3.56 (m, 30 H, O-CH_2), 3.46-3.43 (m, 10 H, O-CH_2), 3.27 (s, 3 H, O-CH_3), 3.26 (s, 9 H, O-CH_3), 3.26 (s, 3 H, O-CH_3), 3.14 (s, 1H, CCH); ^{13}C NMR (500 MHz, $CDCl_3$); δ 164.90, 164.88, 164.84, 138.81, 138.34, 138.31, 135.77, 133.10, 132.81, 132.78, 132.68, 132.47, 131.04, 130.98, 130.91, 130.53, 129.77, 128.51, 123.85, 123.56, 123.53, 123.51, 123.45, 123.39, 123.07, 122.93, 89.91, 88.97, 88.94, 88.90, 88.88, 88.86, 88.19, 81.56, 78.99, 71.85, 70.62, 70.61, 70.57, 70.57, 70.55, 70.54, 7.52, 70.52, 69.06, 68.99, 68.98, 64.52, 64.50, 64.29, 58.90, 24.76; (MALDI)-TOF MS (*trans*-indole acrylic acid matrix): *m/z* = 1475.63 (calcd 1475.59 for $C_{80}H_{92}O_{25}+Na^+$).

Oligomer 8 (H-Ar$_9$-H). TBAF (0.2 mL) was added drop wise to a solution of Compound **6** (0.106 g, 0.04 mmol) in THF (10 mL) the reaction was stirred for 1 min then passed through small plug of silica with 1:1, Acetone: Chloroform solvent mixture then purified by column

chromatography (2:1, Chloroform:Acetone) giving 0.07 g of the product as slightly pale white wax (67 % yield). ^{1}H NMR (500 MHz, $CDCl_3$, 23±2 ^{o}C): δ δ 8.21-8.19 (m, 2H, Ar-H), 8.18-8.16 (m, 14H, Ar-H), 8.12-8.11 (m, 1H, Ar-H), 8.03-8.01 (m, 1H, Ar-H), 7.88-7.86 (m, 6H, Ar-H), 7.85-7.84 (m, 1H, Ar-H), 7.79-7.78 (m, 1H, Ar-H), 7.72-7.70 (m, 1H, Ar-H), 7.44 (dd, 1H, Ar-H J=7.7 Hz), 4.51-4.47 (m, 18H, CO_2-CH), 3.86-3.81 (m, 18H, O-CH), 3.71-3.68 (m, 18H, O-CH), 3.67-3.65 (m, 18H, O-CH_2), 3.63-3.61 (m, 18H, O-CH_2), 3.51-3.49 (m, 18H, O-CH_2), 3.33 (s, 3H, O-CH_3), 3.32(s, 3H, O-CH_3), 3.32 (s, 21H, O-CH_3), 3.14 (s, 1H, CCH); ^{13}C NMR (125 MHz, $CDCl_3$): δ 164.99, 164.94, 138.36, 132.87, 132.79, 132.72, 131.08, 131.05, 123.60, 111.63, 92.09, 89.02, 71.89, 70.65, 70.63, 70.61, 70.57, 69.09, 64.58, 58.98; (MALDI)-TOF MS (*trans*-indole acrylic acid matrix): *m/z* = 2636.01 (calcd 2636.05 for $C_{144}H_{164}O_{45}$+Na^+).

Oligomer 10 (Ar_1-Azo-Ar_1). A mixture of compound **4** (0.19 g, 0.66 mmol), compound **9** (0.13 g, 0.3 mmol), Pd (PPH_3)$_4$ (0.01 g, 0.01 mmol), CuI (0.002 g, 0.012 mmol) and PPh_3 (0.01 g, 0.03 mmol) in dry and degassed diisopropylamine (6 mL) and toluene (2 mL) was heated to 80 °C for 15 hours after which the reaction mixture was concentrated and purified by column chromatography (3:1, Ethyl acetate:hexane) giving 0.15 g of the product as orange solid (65 % yield). ^{1}H NMR (500 MHz, $CDCl_3$, 23±2 ^{o}C): δ 8.22 (dd, *J* = 1.65, *J*=1.2 Hz, 2H, Ar-H), 8.02 (dd, *J* = 7.8, *J* = 1.2, Hz, 2H, Ar-H), 7.92 (d, *J* = 8.6 Hz, 4H, Ar-H), 7.71 (dd, *J* = 7.7, *J* = 1.6, 2H, Ar-H), 7.67 (d, *J* = 8.6, 4H, Ar-H), 7.43 (dd, *J* = 7.8, *J* = 7.7 Hz, 2H, Ar-H), 4.47 (t, *J* = 4.8, Hz 4 H, CO_2-CH_2), 3.80-3.76 (m, 4 H, O-CH_2), 3.66-3.56 (m, 12 H, O-CH_2), 3.46-3.43 (m, 4 H, O-CH_2), 3.27 (s, 6 H, O-CH_3); ^{13}C NMR (125 MHz, $CDCl_3$): δ 165.75, 151.94, 135.78, 132.87, 13251, 130.54, 129.67, 128.53, 125.81, 123.36, 123.07, 90.98, 90.00, 71.91, 70.69, 70.63, 70.60, 69.15, 64.34, 58.98. EI-MS (80 eV, 90 °C): *m/z* = 762.3 (calcd 762.3 for $C_{44}H_{46}O_{10}N_2^+$), Anal. C: 68.81, H: 5.94, N: 2.91 (calcd C: 69.28, H: 6.08, N: 3.67).

Oligomer 11 (Ar_5-Azo-Ar_5). Free acetylene **7** (0.33 g, 0.23 mmol), compound **9** (0.048, 0.11 mmol), Pd (PPH_3)$_4$ (0.03 g, 0.03 mmol), CuI (0.002 g, 0.012 mmol) and PPh_3 (0.01g, 0.03 mmol) were suspended in toluene (5 mL) and diisopropylamine (10 mL) and heated to 70 °C for 17 hours. the reaction mixture was concentrated under vacuum and purified by column chromatography (1:3, Acetone:Dichloromethane) resulting in 0.1 g of the product as orange wax (30 % yield). ^{1}H NMR (500 MHz, $CDCl_3$, 23±2 ^{o}C) δ; 8.21-8.17 (m, 18H, Ar-H), 8.04-8.02 (m, 2H, Ar-H), 7.95-7.93 (m, 4H, Ar-H), 7.90-7.88 (m, 8H, Ar-H), 7.72-7.68 (m, 6H, Ar-H), 7.45-7.42 (m, 2H, Ar-H), 4.51-4.47 (m, 20H, CO_2-CH), 3.86-3.81 (m, 20H, O-CH_2), 3.71-3.61 (m, 60

H, O-CH_2), 3.51-3.49 (m, 20H, O-CH_2), 3.33-3.32 (m, 30H, O-CH_3); ^{13}C NMR (125 MHz, $CDCl_3$): δ 169.66, 165.02, 164.96, 162.87, 138.38, 135.82, 132.86, 132.76, 132.60, 130.58, 128.55, 123.90, 123.13, 123.12, 109.73, 104.34, 102.78, 92.53, 89.96, 89.09, 88.23, 71.90, 71.89, 70.66, 70.63, 70.62, 70.59, 70.57, 69.11, 69.05, 64.56, 58.95, 30.84; GPC: 4265 (Mn), 1.01 (Mw/Mn); (MALDI)-TOF MS (*trans*-indole acrylic acid matrix): *m/z* = 3106.52 (calcd 3106.23 for $C_{172}H_{190}O_{50}$+Na^+).

Oligomer 12 (Ar_9-Azo-Ar_9). Oligomer **8** (0.11 g, 0.04 mmol), compound **9** (0.01, 0.02 mmol), Pd $(PPH_3)_4$ (0.02 g, 0.02 mmol), CuI (0.002 g, 0.012 mmol) and PPh_3 (0.01g, 0.03 mmol) were dissolved in a solvent mixture of diisopropylamine (3 mL), toluene (1.2 mL) and tetrahydrofuran (0.5 mL) and stirred for 16 hours at 80 °C then concentrated under reduced pressure and purified by column chromatography (2:3, 1:1 Acetone:Chloroform) then 5:1 Chloroform:Isopropanol giving 0.05 g of the product as orange wax (46 % yield). ^{1}H NMR (500 MHz, $CDCl_3$, 23±2 ^{o}C) δ; 8.22-8.18 (m, 32H, Ar-H), 8.05-8.03 (m, 2H, Ar-H), 7.96-7.94 (m, 3H, Ar-H), 7.90-7.89 (m, 19H, Ar-H), 7.73-7.69 (m, 6H, Ar-H), 7.46-7.43 (m, 2H, Ar-H), 4.51-4.47 (m, 36H, CO_2-CH), 3.86-3.81 (m, 36H, O-CH_2), 3.71-3.61 (m, 108 H, O-CH_2), 3.51-3.49 (m, 36H, O-CH_2), 3.33 (s, 9H, O-CH_3), 3.32(s, 45H, O-CH_3); ^{13}C NMR (125 MHz, $CDCl_3$): δ 172.68, 164.96, 138.36, 135.26, 132.87, 132.81, 132.61, 131.10, 128.56, 124.26, 123.60, 123.13, 89.02, 88.25, 71.91, 70.68, 70.67, 70.64, 60.63, 70.62, 70.60, 69.12, 69.05, 64.58, 64.34, 58.96. GPC: 6592 (Mn), 1.03 (Mw/Mn); (MALDI)-TOF MS (*trans*-indole acrylic acid matrix): *m/z* = 5429.53 (calcd 5429.17 for $C_{300}H_{336}O_{90}N_2$+Na^+).

Azobenzene Diacid 14. Methyl 3-bromo-5-nitrobenzoate **13** (0.52 g, 2 mmol) was dissolved in ethanol (10 mL) and water (5 mL). NaOH (0.3 g, 8 mmol) and Zn (0.26 g, 4 mmol) were added and the reaction mixture was refluxed at for 20 hours. The resulting solution was diluted with water then neutralized with 1M HCl and filtered. The resulting orange solid was washed with plenty of water to give 0.6 g of product as orange solid (70 % yield). ^{1}H-NMR (500 MHz, DMSO): δ 8.38 (dd, *J* = 1.5, 1.5 Hz, 2 H, Ar-H), 8.33 (dd, *J* = 1.5, 1.5 Hz, 2 H, Ar-H), 8.21 (dd, *J* = 1.5, 1.5 Hz, 2 H, Ar-H); ^{13}C- NMR (125 MHz, DMSO); δ 165.48, 152.70, 134.84, 134.40, 129.63, 122.95; EI-MS (80 eV, 90 °C): *m/z* = 425.7 (calcd 425.8 for $C_{14}H_8N_2O_4Br_2^+$). Anal. C: 38.40, H: 1.98, N: 6.08 (calcd C: 39.28, H: 1.88, N: 6.54).

Azobenzene Bis(Chiral Glyme Ester) 16. Bis-acid **14** (0.34 g, 0.8 mmol) was mixed with thionyl chloride (25 mL) and refluxed for 2 h. Excess thionyl chloride was removed *in vacuo* and

the remaining residue was dried on a vacuum pump for 3 h to afford the crude acid chloride as a orange solid. It was then added to a stirring solution of chiral alcohol **15** (0.53 mL, 2 mmol) and triethylamine (0.4 mL, 4 mmol) in 10 mL of CH_2Cl_2 at 0 °C. The suspension was allowed to warm to room temperature and stirred overnight. Then the organic layer was washed with brine and sat. aq. NH_4Cl solution. The residue was purified by column chromatography (6:1, DCM:Acetone) to yield 0.4 g of the product as a red oil (60 % yield); ^{1}H-NMR (500 MHz, $CDCl_3$): δ 8.49 (dd, *J* = 1.8, 1.8 Hz, 2 H, Ar-H), 8.24 (dd, *J* = 1.8, 1.8 Hz, 2 H, Ar-H), 8.17 (dd, *J* = 1.8, 1.8 Hz, 2 H, Ar-H), 5.40-5.28 (m, COO-CH, 2H), 3.72-3.54 (m, 24 H, O-CH_2), 3.50-3.44 (m, 4H, O-CH_2), 3.30 (s, 6 H, O-CH_3), 1.35 (d, *J* = 6.37 Hz, 6H, C-CH_3); ^{13}C- NMR (125 MHz, $CDCl_3$); δ 163.91, 152.71, 135.01, 133.41, 128.27, 124.55, 123.07, 73.52, 71.83, 71.02, 70.75, 70.53, 70.40, 58.87, 16.64; FAB-MS (MNBA, 3 kV): *m/z* = 859 (calcd 859 for $C_{34}H_{48}N_2O_{12}Br_2Na^+$).

Oligomer 17 (Ar_1-Azo-Ar_1). Dry and degassed acetonitrile (0.5 mL), diisopropylamine (1 mL) and toluene (0.5 mL) were added to a mixture of compound **16** (0.14 g, 0.17 mmol), **4** (0.11 g, 0.37 mmol), $Pd(PPh_3)_4$ (0.01 g, 0.01 mmol), CuI (0.003 g, 0.01 mmol), and PPh_3 (0.005 g, 0.01 mmol). The flask was sealed and heated to 80 °C for 22 hours. The reaction mixture was diluted with ethylacetate, filtered, concentrated and purified by column chromatography (1:4, acetone:dichloromethane) to give 0.1 g (46 % yield) of the product; ^{1}H-NMR (500 MHz, $CDCl_3$): δ 8.56 (dd, *J* = 1.65, 1.79 Hz, 2 H, Ar-H), 8.31 (dd, *J* = 1.65, 1.51 Hz, 2 H, Ar-H), 8.26 (dd, *J* = 1.65, 1.79 Hz, 2 H, Ar-H), 8.24 (t, *J* = 1.24, 2 H, Ar-H), 8.05-8.03 (m, 2H, Ar-H), 7.75-7.73 (m, 2H, Ar-H), 7.45 (t, *J* = 7.8 Hz, 2H, Ar-H), 5.43-5.37 (m, COO-CH, 2H), 4.49 (t, *J* = 4.95 Hz, 4 H, O-CH_2), 3.84 (t, *J* = 4.81 Hz, 4 H, O-CH_2), 3.76-3.69 (m, 10H, O-CH_2), 3.67-3.62 (m, 22H, O-CH_2), 3.60-3.57 (m, 8H, O-CH_2); 3.51-3.47 (m, 8H, O-CH_2), 3.32 (s, 6H, O-CH_3), 3.30 (s, 6H, O-CH_3), 1.39 (d, *J* = 6.46 Hz, 6H, C-CH_3); ^{13}C- NMR (125 MHz, $CDCl_3$); δ165.62, 164.55, 152.12, 135.81, 132.18, 130.50, 128.52, 124.34, 122.90, 89.99, 88.39, 73.57, 71.82, 71.79, 70.73, 70.60, 70.55, 70.50, 70.38, 69.05, 64.27, 58.91, 58.90, 58.88, 16.74; GPC: 1857 (Mn), 1.00 (Mw/Mn); (MALDI)-TOF MS (*trans*-indole acrylic acid matrix): *m/z* = 1281.64 (calcd 1282.28 for $C_{66}H_{86}O_{22}N_2$+Na^+).

Oligomer 18 (Ar_5-Azo-Ar_5). Dry and degassed acetonitrile (1 mL), diisopropylamine (1 mL) and toluene (0.5 mL) were added to a mixture of compound **16** (0.15 g, 0.18 mmol), **7** (0.55 g, 0.37 mmol), $Pd(PPh_3)_4$ (0.01 g, 0.01 mmol), CuI (0.003 g, 0.01 mmol), and PPh_3 (0.005 g, 0.01

mmol). The flask was sealed and heated to 80 °C for 22 hours. The reaction mixture was diluted with ethylacetate, filtered, concentrated and purified by column chromatography (0.3:1:9, Methanol:Acetone:Dichloromethane) to give 0.3 g (46 % yield) of the product; ^{1}H-NMR (500 MHz, $CDCl_3$): δ 8.56 (dd, *J* = 1.65, 1.79 Hz, 2 H, Ar-H), 8.30 (dd, *J* = 1.65, 1.51 Hz, 2 H, Ar-H), 8.26 (dd, *J* = 1.65, 1.79 Hz, 2 H, Ar-H), 8.20 (t, *J* = 1.24, 2 H, Ar-H), 8.18-8.14 (m, 14 H, Ar-H), 8.01-7.99 (m, 2H, Ar-H), 7.90 (t, *J* = 1.51 Hz, 2H, Ar-H), 7.87-7.85 (m, 8H, Ar-H), 7.69-7.67 (m, 2 H, Ar-H), 7.45 (t, *J* = 7.7 Hz, 2H, Ar-H), 5.40-5.36 (m, COO-CH, 2H), 4.48-4.44 (m, 20 H, O-CH_2), 3.85-3.79 (m, 24 H, O-CH_2), 3.72-3.54 (m, 84 H, O-CH_2), 3.49-3.45 (m, 20H, O-CH_2), 3.31-3.29 (m, 36H, O-CH_3), 1.39 (d, *J* = 6.46 Hz, 6H, C-CH_3); ^{13}C- NMR (125 MHz, $CDCl_3$); 165.62, 164.96, 164.91, 164.50, 152.18, 138.31, 135.79, 135.13, 132.82, 132.75, 132.71, 132.67, 132.49, 132.29, 1321.05, 131.04, 131.02, 130.97, 130.51, 129.78, 129.03, 128.52, 125.00, 124.06, 123.84, 123.56, 123.53, 123.45, 122.93, 89.92, 89.05, 88.98, 88.96, 88.87, 88.20, 73.59, 71.85, 71.82, 70.78, 70.75, 70.61, 70.58, 70.57, 70.54, 70.53, 70.41, 69.06, 69.00, 64.52, 64.50, 64.29, 58.92, 58.91, 58.90, 53.36, 16.77; GPC; 4101 (Mn), 1.01 (Mw/Mn); (MALDI)-TOF MS (*trans*-indole acrylic acid matrix): *m/z* = 3602.25 (calcd 3602.38 for $C_{194}H_{230}O_{62}N_2$+Na^+).

Methyl 2-methoxy-5-nitrobenzoate 19. 5-Nitrosalicylic acid (18.3 g, 100 mmol) was dissolved in DMF (250 mL) then K_2CO_3 (41.4 g, 300 mmol) was added in small portions followed by MeI (70 mL, 500 mmol). The reaction mixture was heated to 100 °C for 30 min then cooled down to room temperature, and poured into 1 L of water. The resulting precipitate was collected by filtration and recrystallized from ethanol giving 18 g of the product as a white solid (85% yield). ^{1}H-NMR (300 MHz, $CDCl_3$): δ 8.67 (d, *J* = 2.9 Hz, 1 H, Ar-H), 8.34 (dd, *J* = 9.1 and 2.9 Hz, 1 H, Ar-H), 7.04 (d, *J* = 9.1 Hz, 1 H, Ar-H), 3.99 (s, 3 H, O-CH_3), 3.91 (s, 3 H, O-CH_3); ^{13}C- NMR (300 MHz, $CDCl_3$); δ 164.84, 164.00, 141.05, 129.28, 128.19, 120.86, 112.38, 57.20, 52.93; EI-MS (80 eV, 60 °C): *m/z* = 211 (calcd 211.1 for $C_9H_9NO_5^+$).

Methyl 3-bromo-2-methoxy-5-nitrobenzoate 20. Methyl 2-methoxy-5-nitrobenzoate **19** (3.1 g, 15 mmol) was dissolved in conc. sulfuric acid (100 mL) at 0 °C and DIB[3] (4.3 g, 15 mmol) was added in small amounts. The reaction mixture was stirred at room temperature for 3 h and then poured on ice resulting in a yellow precipitate, which was recrystallized from ethanol furnishing 3.5 g of the product as a white solid (80% yield). ^{1}H-NMR (300 MHz, $CDCl_3$): δ 8.61 (d, *J* = 2.7 Hz, 1 H, Ar-H), 8.57 (d, *J* = 2.7 Hz, 1 H, Ar-H), 4.00 (s, 3 H, O-CH_3), 3.96 (s, 3 H, O-CH_3); ^{13}C-

NMR (300 MHz, $CDCl_3$); δ 163.77, 162.00, 131.85, 126.65, 126.12, 119.78, 62.73, 53.07; EI-MS (80 eV, 55 °C): *m/z* = 289 (calcd 290 for $C_9H_8NBrO_5^+$).

Methyl 3-bromo-2-methoxy-5-aminobenzoate 21. Methyl 3-bromo-2-methoxy-5-nitrobenzoate **20** (2 g, 7 mmol) was dissolved in 20 mL of ethanol, then $SnCl_2 \cdot 2H_2O$ (7.8 g, 35 mmol) was added, and the reaction mixture was heated to 80 °C for 1 h. It was then poured on ice and the solution was adjusted to pH = 8 by addition of 1 N NaOH. The aqueous layer was extracted with ethyl acetate, the combined organic layers were washed with water and brine, and the solvent was removed under reduced pressure giving 1.5 g product as a yellow oil. (82% yield). ^{1}H-NMR (300 MHz, $CDCl_3$): 7.06 (s, 2 H, Ar-H), 3.88 (s, 3 H, O-CH_3), 3.81 (s, 3 H, O-CH_3); ^{13}C- NMR (300 MHz, $CDCl_3$); δ 166.00, 158.00, 126.63, 123.53, 119.48, 116.91, 62.13, 52.42; EI-MS (80 eV, 65 °C): *m/z* = 259 (calcd 260 for $C_9H_{10}NBrO_3^+$).

Azobenzene Bis(methyl ester) 22. Methyl 3-bromo-2-methoxy-5-aminobenzoate **21** (1.3 g, 5 mmol) was dissolved in pyridine (50 mL) then CuI (4.7 g, 25 mmol) was added and the reaction mixture was stirred at room temperature for 3 d. The reaction mixture was diluted with ethyl acetate then passed through a short plug of silica gel, subsequently washed with water, brine, 1 N HCl, and again with water and brine. The organic layer was removed under reduced pressure and purified by column chromatography (ethyl acetate:hexanes = 1:9) giving 0.5 g of the product as orange solid (19% yield). ^{1}H-NMR (300 MHz, $CDCl_3$): δ 8.33 (d, *J* = 2.5 Hz, 2 H, Ar-H), 8.26 (d, *J* = 2.5 Hz, 2 H, Ar-H), 3.98 (s, 3 H, O-CH_3), 3.96 (s, 3 H, O-CH_3); ^{13}C- NMR (300 MHz, $CDCl_3$); δ 165.38, 159.53, 148.40, 130.26, 127.30, 120.59, 62.84, 53.08; EI-MS (80 eV, 160 °C): *m/z* = 516 (calcd 516.1 for $C_{18}H_{16}N_2Br_2O_6^+$).

Azobenzene Diacid 23. Compound **22** (0.18 g, 0.35 mmol) was dissolved in THF (2 mL), diluted with 1 N NaOH (50 mL), and then refluxed at 80 °C for 3 h. The dark red reaction mixture was neutralized with concentrated HCl. The resulting orange solid was washed with plenty of water to give 0.15 g of the product as an orange solid (87% yield). ^{1}H-NMR (300 MHz, D_2O): δ 8.08 (d, 2 H, Ar-H), 7.84 (d, 2 H, Ar-H), 3.92 (s, 6 H, O-CH_3); ^{13}C- NMR (300 MHz, D_2O); δ 170.00, 155.00, 150.00, 135.00, 126.73, 123.31, 96.04, 62.36; EI-MS (80 eV, 270 °C): *m/z* = 488 (calcd 488 for $C_{16}H_{12}N_2Br_2O_6^+$).

Azobenzene Bis(Chiral Glyme Ester) 24. Compound **23** (0.43 g, 0.9 mmol) was suspended in thionyl chloride (50 mL) and refluxed for 2 h. Excess thionyl chloride was removed *in vacuo* and the remaining residue was dried on a vacuum pump for 3 h to afford the crude acid chloride as a

red solid, which was subsequently added to a stirring solution of chiral alcohol **15** (0.5 mL, 2.2 mmol), triethylamine (0.45 mL, 4.5 mmol), and 4-dimethylaminopyridine (DMAP; 0.004 g, 0.04 mmol) in 15 mL of CH_2Cl_2 at 0 °C. The suspension was allowed to warm to room temperature and stirred overnight. Then the organic layer was washed with brine and sat. aq. NH_4Cl solution. The residue was purified by column chromatography (ethyl acetate:hexanes = 2:1) to yield 0.55 g of the product as an orange oil (51% yield). ^{1}H-NMR (300 MHz, $CDCl_3$): δ 8.29 (d, *J* = 2.4 Hz, 2 H, Ar-H), 8.23 (d, *J* = 2.4 Hz, 2 H, Ar-H), 5.4-5.35 (m, 2 H, CO_2-CH), 3.98 (s, 6 H, O-CH_3), 3.72-3.58 (m, 24 H, O-CH_2), 3.51-3.48 (m, 4 H, O-CH_2), 3.33 (s, 6 H), 1.38 (d, *J* = 6.4 Hz, 6 H); ^{13}C- NMR (300 MHz, $CDCl_3$); δ 164.23, 158.92, 147.97, 129.06, 127.53, 127.40, 120.07, 73.56, 71.89, 70.98, 70.75, 70.62, 70.59, 70.48, 62.46, 58.98, 16.67; EI-MS (80 eV, 245 °C): *m/z* = 896 (calcd 896.6 for $C_{36}H_{52}N_2Br_2O_{14}^+$).

Azobenzene Bis(TMSacetylene) 25. Dry and degassed diisopropylamine (1 mL) and toluene (0.5 mL) were added to a mixture of compound **24** (0.035 g, 0.4 mmol), trimethylsilylacetylene (TMSA; 0.4 g, 4 mmol), $Pd(PPh_3)_4$ (0.028 g, 0.02 mmol), CuI (0.008 g, 0.04 mmol), and PPh_3 (0.005 g, 0.02 mmol). The flask was sealed and heated to 60 °C for 24 h. The reaction mixture was diluted with ethylacetate, filtered, concentrated and purified by column chromatography (ethyl acetate:hexanes = 3:1) to give 0.12 g of the product as an orange oil (31% yield). ^{1}H-NMR (300 MHz, $CDCl_3$): δ 8.22 (d, *J* = 2.4, Hz, 2 H, Ar-H), 8.08 (d, *J* = 2.4, Hz, 2 H, Ar-H), 5.37-5.31 (m, CO_2-CH, 2H), 4.15 (s, 6H, Ar-OCH_3), 3.69-3.49 (m, 24 H, O-CH_2), 3.49-3.47 (m, 4 H, O-CH_2), 3.33 (s, 6 H, O-CH_3), 1.36 (d, *J* = 6.39 Hz, 6H, C-CH_3), 0.23 (s, 18H, Si-CH_3); ^{13}C- NMR (125 MHz, $CDCl_3$); 164.79, 163.07, 147.23, 130.37, 126.83, 126.77, 119.43, 101.12, 99.68, 73.58, 71.87, 70.74, 70.61, 70.58, 70.47, 62.07, 58.99, 16.73, 0.26; ESI (pos) MS: *m/z* = 953.4 (calcd 953.4 for $C_{46}H_{70}O_{14}N_2Si_2$+$Na^+$).

Azobenzene Diiodide 28. Compound **25** (0.074 g, 0.08 mmol) was dissolved in 5 mL of THF and 1 mL of TBAF was added. The reaction mixture was stirred at room temperature for 1 min and then filtered through a short plug of silica gel using ethyl acetate as solvent. The solvent was removed under reduced pressure yielding 0.063 g of terminal bisacetylene **25** as an orange wax, which was used without further characterization. Dry and degassed diisopropylamine (6 mL) and toluene (2 mL) were then added to a mixture of bisacetylene **25** (0.063 g, 0.08 mmol), diiodide **27** (0.8 g, 1.6 mmol), $Pd(PPh_3)_4$ (0.028 g, 0.1 mmol), CuI (0.008 g, 0.04 mmol) and PPh_3 (0.01 g, 0.02 mmol). The flask was sealed and heated to 60 °C for 2 h to dissolve all the diiodide

monomer then heating was turned off and the reaction was stirred at room temperature for 12 hours. The reaction mixture was diluted with ethyl acetate, filtered, concentrated, and purified by column chromatography involving a gradient (ethyl acetate:hexanes = 2:1 → methanol:ethyl acetate = 0.1:1 → 3:1) to give 0.04 g (32 % yield) of the product as orange wax. ^{1}H-NMR (300 MHz, $CDCl_3$): δ 8.30 (dd, *J* = 1.6, 1.2 Hz, 2 H, Ar-H), 8.27 (d, *J* = 2.7, Hz, 2 H, Ar-H), 8.14 (d, *J* = 2.7, Hz, 2 H, Ar-H), 8.13 (d, *J* = 1.6, 1.2 Hz, 2 H, Ar-H), 8.02 (dd, *J* = 1.6, 1.2 Hz, 2 H, Ar-H), 5.37-5.31 (m, CO_2-CH, 2H), 4.46-4.43 (m, 4 H, CO_2-CH_2), 4.08 (s, 6H, Ar-O-CH_3), 3.82-3.72 (m, 4 H, O-CH_2), 3.66-3.53 (m, 38 H, O-CH_2), 3.49-3.44 (m, 8 H, O-CH_2), 3.30 (s, 6 H, O-CH_3), 3.28 (s, 6 H, O-CH_3), 1.36 (d, *J* = 6.4 Hz, 6H, C-CH_3); ^{13}C- NMR (125 MHz, $CDCl_3$); 164.71, 164.35, 162.84, 147.44, 144.03, 138.56, 132.09, 131.93, 130.13, 127.38, 126.90, 125.04, 118.91, 93.32, 92.20, 86.65, 73.63, 71.95, 71.92, 70.84, 70.80, 70.69, 70.66, 70.62, 70.50, 69.05, 64.70, 82.58, 59.02, 58.99, 16.76; ESI (pos) MS: *m/z* = 1571.4 (calcd 1571.3 for $C_{68}H_{88}O_{24}N_2I_2^+$).

Oligomer 29. Dry and degassed diisopropylamine (0.5 mL) and toluene (0.5 mL) were added to a mixture of diiodide **10** (7 mg, 0.009 mmol), pentamer acetylene **7** (14 mg, 0.018 mmol), $Pd(PPh_3)_4$ (0.01 g, 0.01 mmol), CuI (0.003 g, 0.01 mmol), and PPh_3 (0.005 g, 0.01 mmol). The flask was sealed and heated to 60 °C for 12 h. The reaction mixture was then diluted with ethyl acetate, filtered, concentrated, and purified by column chromatography involving a gradient (CH_2Cl_2:acetone = 3:1 → acetone → methanol:acetone = 0.1:10) to give 10 mg of the desired product (52 % yield). For all analytical measurements, the product was further purified by prep. GPC. ^{1}H-NMR (300 MHz, $CDCl_3$, Figure 7): δ 8.31 (d, *J* = 2.46 Hz, 2 H, Ar-H), 8.22-8.17 (m, 24 H, Ar-H), 8.05-8.01 (dt, *J* = 1.2, 7.7 Hz, 2 H, Ar-H), 7.89-7.87 (m, 10 H, Ar-H), 7.72-7.69 (dt, *J* = 1.2, 7.7 Hz, 2 H, Ar-H), 7.44 (t, *J* = 7.7 Hz 2 H, Ar-H), 5.41-5.35 (m, 2 , CO_2-CH), 4.52-4.49 (m, 24 H, CO_2-CH_2), 4.15 (s, 6 H, O-CH_3), 3.86-3.83 (m, 24 H, O-CH_2), 3.70-3.62 (m, 100 H, O-CH_2), 3.52-3.49 (m, 24 H, O-CH_2), 3.33 (s, 10 H, O-CH_3), 3.31 (s, 32 H, O-CH_3), 1.39 (d, *J* = 6.4 Hz, 6 H, C-CH_3); GPC (THF, 30 ^{o}C, Figure 8): M_w = 9500, PDI (M_w/M_n) = 1.0; ESI (pos) MS (Figure 9): *m/z* = 2134 (calcd 2134 for $C_{228}H_{270}O_{74}N_2$+2Na^{++}), 1430 (calcd 1430 for $C_{228}H_{270}O_{74}N_2$+3Na^{+++}).

References

1 D. G. Hill, M. J. Mio, R. B. Prince, T. S. Hughes, J. S. Moore, *Chem. Rev*. **2001,** *101*, 3893.

2 *Photochromism - Molecules and Systems,* (Eds.: H. Dürr, H. Bouas-Laurent), Elsevier: Amsterdam, **2003**; (b) *Molecular Switches*, (Ed.: B. L. Feringa), Wiley: Weinheim, **2001**; (c) Special Issue: „Photochromism: Memories and Switches"; *Chem. Rev.* **2000**, *100*, 1683, and references therein.

3 V. Balzani, A. Credi, M. Venturi, *Molecular Devices and Machines:* A Journey into the Nanoworld, Wiley-VCH, Weinheim, **2003**.

4 (a) O. Pieroni, A. Fissi, N. Angelini, F. Lenci, *Acc. Chem. Res.* **2001**, *34*, 9.

5 F. Ciardelli, D. Fabbri, O. Pieroni, A. Fissi, *J. Am. Chem. Soc.* **1989**, *111*, 3470.

6 F. Ciardelli, O. Pieroni, A. Fissi, J. L. Houben, *Biopolymers.* **1984**, *23*, 1423.

7 O. Pieroni, A. Fissi, F. Ciardelli, *Biopolymers.* **1987**, *26*, 1993.

8 G. A. Woolley, *Acc. Chem. Res.* **2005**, *38*, 486.

9 D. J. Flint, J. R. Kumita, O. S. Smart, G. A. Woolley, *Chemistry & Biology*. **2002**, *9*, 391.

10 J. C. Nelson, J. G. Saven, J. S. Moore, P. G. Wolynes, *Science*. **1997**, *277*, 1793.

11 R. B. Prince, J. G. Saven, P. G. Wolynes, J. S. Moore, *J. Am. Chem. Soc.* **1999**, *121*, 3114.

12 K. Matsuda, M. T. Stone, J. S. Moore, *J. Am. Chem. Soc.* **2002**, *124*, 11836.

13 D. J. Hill, J. S. Moore, *Proc Natl. Acad. Sci.* **2002**, *99*, 5053.

14 R. B. Prince, Ph.D thesis, University of Illinois at Urbana-Champaign, Urbana, IL, **2000**.

15 R. B. Prince, T. Okada, J. S. Moore, *Angew. Chem. Int. Ed. Engl*. **1999,** *38*, 233.

16 (a) J. M. Cary, J. S. Moore, *Org. Lett.* **2002**, *4*, 4663. (b) X. Yang, A L Brown, M. Furukawa, S. Li, W. E. Gardinier, E. J. Bukowski, F. V. Bright, C. Zheng, X. C. Zeng, B. Gong, *Chem. Commun.* **2003,** 56.

17 For the most prominent examples, consult: (a) S. Lahiri, J. L. Thompson, J. S. Moore, *J. Am. Chem. Soc.* **2000**, *122*, 11315. (b) H. Goto, J. M. Heemstra, D. J. Hill, J. S. Moore, *Org. Lett.* **2004**, *6*, 889.

18 For the use of (*S*)-β-methyl-tri(ethyleneglycol) side chains, see: (a) R. B. Prince, L. Brunsveld, E. W. Meijer, J. S. Moore, *Angew. Chem. Int. Ed. Engl.* **2000**, *39*, 228. (b) R. B. Prince, J. S. Moore, L. Brunsveld, E. W. Meijer, *Chem. Eur. J.* **2001**, *7*, 4150.

19 For example, see: L.-X. Liao, F. Stellacci, D. V. McGrath, *J. Am. Chem. Soc.* **2004**, *126*, 2181.

20 R. B. Prince, L. Brunsveld, E. W. Meijer, J. S. Moore, *Angew. Chem. Int. Ed. Engl.* **2000,** *39*, 228.

21 L. Brunsveld, R.B. Prince, E. W. Meijer, J. S. Moore, *Org. Lett.* **2000,** *2*, 1525.

22 R. B. Prince, S. A. Barnes, J. S. Moore, *J. Am. Chem. Soc*, **2000**, *122*, 2758.

23 M. S. Gin, J. S. Moore, *Org. Lett*. **2000,** *2*, 135.

24 M. S. Gin, T. Yokozawa, R. B. Prince, J. S. Moore, *J. Am. Chem. Soc.* **1999**, *121*, 2643.

25 J. Zhang, D. J. Pesak, J. L. Ludwick, J. S. Moore, *J. Am. Chem. Soc*. **1994**, *116*, 4227.

26 D. G. Koehler, D. Liu, S. D. Feyter, V. Enkelmann, T. Weil, C. Engels, C. Samyn, K. Mullen, C. D. Schryver, *Macromolecules.* **2003**, *36*, 578.

27 C. Kaiser, Ph.D thesis, Freie.Universität Berlin.

28 A. Khan, S. Hecht, *Chem. Commun*. **2004**, 300.